Characterization of 3 different types of aquaporins in *Carcinus maenas* and their potential role in osmoregulation

By

Mikyla Tara Nash

A Thesis submitted to the Faculty of Graduate Studies of
The University of Manitoba
in partial fulfillment of the requirements of the degree of

MASTER OF SCIENCE

Department of Biological Sciences

University of Manitoba

Winnipeg

Abstract

Intertidal crustaceans like *Carcinus maenas* shift between an osmoconforming and osmoregulating state when inhabiting full-strength seawater and dilute environments, respectively. While the bodily fluids and environment of marine osmoconformers are approximately isosmotic, osmoregulating crabs inhabiting dilute environments maintain their bodily fluid osmolality above that of their environment by actively absorbing and retaining osmolytes (e.g., Na^+, Cl^-, urea) while eliminating excess water. Few studies have investigated the role of aquaporins (AQPs) in the osmoregulatory organs of crustaceans, especially within brachyuran species. In the current study, three different aquaporins were identified within a transcriptome of *C. maenas*, including a classical AQP (CmAQP1), an aquaglyceroporin (CmGLP1), and a big-brain protein (CmBIB1), all of which are expressed in the gills and the antennal glands. Functional expression of these aquaporins confirmed water transport capabilities for CmAQP1, CmGLP1, but not for CmBIB1, while CmGLP1 also transported urea. Higher relative CmAQP1 mRNA expression within tissues of osmoconforming crabs suggests the apical/sub-apically localized channel attenuates osmotic gradients created by non-osmoregulatory processes while its downregulation in dilute media reduces the water permeability of tissues to facilitate osmoregulation. Although hemolymph urea concentrations rose upon exposure to brackish water, urea was not detected in the final urine. Due to its urea-transport capabilities, CmGLP1 is hypothesized to be involved in a urea retention mechanism believed to be involved in the production of diluted urine. Overall, these results suggest that AQPs are involved in osmoregulation and provide a basis for future mechanistic studies investigating the role of AQPs in volume regulation in crustaceans.

Acknowledgments

First and foremost, I would like to thank my wonderful advisor, Dr. Dirk Weihrauch for his continuous encouragement, patience, and his belief in me as a student. Dirk is always eager to dedicate his time to helping students pursue their ideas and passions while providing all the opportunities available to collaborate and network with members of our research community. Dirk has provided an endless amount of support both professionally and personally throughout my years in his lab and for this, I am forever grateful. I would not be the person I am today without you.

I would also like to thank my committee members Dr. Jason Treberg and Dr. Kenneth Jeffries for going above and beyond their duties and for their continuous guidance along the way. I would like to express my gratitude to my collaborator Dr. Jonathan Wilson. I would also like to thank my funding sources, NSERC, Graduate Enhancement of Tri-Agency Stipends, and Science Enhancement of Grant Stipends, without them, this thesis would not be possible.

To past and present members of the Crab Lab, thank you for all your technical and moral support through both the highs and lows of this thesis. I have gained a second family through you all and I am so happy to have been a part of your lives. Maria, I will forever treasure the special bond that we share, and I am incredibly grateful for all the support you have given me through the years. Alex, you have provided countless examples of what it means to be both a good friend and a good lab mate. Your expert advice and support are deeply appreciated.

I would also like to thank all my friends and family. Your unwavering support throughout the years does not go unnoticed. You have continuously encouraged me to make my own choices that make me happy. I would like to express my deepest gratitude to you all. Garett, you have seen all the highs and lows of this journey. Thank you for celebrating the highs with me, helping me pick myself back up during the lows, and for all your help along the way. To my parents, I don’t know if you were really prepared for a child with a million questions about the world around them, but I am eternally grateful for all your patience in answering all my questions a million times over. You have allowed me to ignite a passion to continue to ask and hopefully answer many more questions.

Dedication

My time as a graduate student has provided me with some of the greatest friendships and experiences to date. This journey has been incredibly transformative. I was able to accomplish things that I only thought I could dream of doing. Although this time has often been filled with joy and excitement, it also included times of great sorrow. Towards the beginning of my degree, I lost my dear friend Brittany Brook. Brittany was also a graduate student at the University of Manitoba, but our friendship began long before graduate school. Brittany was one of the main reasons I decided to pursue my degree. She encouraged me to follow my dreams and was always there to chase away any self-doubt. Brittany's passion for animals and her devotion to answering questions to promote their well-being was incredibly inspiring. Her death is a huge loss that I still struggle to come to terms with. She was an extraordinarily kind and talented woman who is greatly missed. I know she would have been proud of what I have accomplished and would be excited to see what is still yet to come.

I would like to dedicate this dissertation to Brittany Catherine Brook.

Carpe Diem

Thesis Contributions

A condensed form of this thesis has been accepted in the journal of Comparative Biochemistry and Physiology, Part A (https://doi.org/10.1016/j.cbpa.2022.111281).

Author contributions:

Mikyla Tara Nash designed the study, performed experiments, analyzed data, and wrote the manuscript. Alex Renaldo Quijada-Rodriguez aided in experiments and revised the manuscript. Garett Joseph Patrick Allen aided in experiments and revised the manuscript. Dr. Jonathan Wilson performed and analyzed data pertaining to immunohistochemical localization of *Carcinus maenas* AQP1 and revised the manuscript. Dirk Weihrauch, revised the manuscript, assisted with study design and provided financial assistance.

Table of Contents

List of Tables

List of Figures

1.0 Introduction

1.1 Cell Volume regulation

Maintaining cell volume homeostasis is an essential physiological process shared by all living cells. Cells face osmotic stress upon changes in the osmolality of their respective extracellular fluids (e.g., water, blood, hemolymph, urine). Upon an osmotic challenge, cell volume is regulated through physiological mechanisms that adjust their concentration of intracellular inorganic and organic solutes, termed osmolytes. These adjustments are made through the activation of membrane transporters and/or metabolic processes, as described below, that balance the amount of osmolytes and water within the cell to reduce osmotic pressures without disrupting cell integrity, a process referred to as anisosmotic cell volume regulation (Chamberlin and Strange, 1989).

Cell volume regulatory responses involving the loss or gain of osmolytes are termed a regulatory volume decrease and regulatory volume increase, respectively (Fig. 1). These osmolytes are primarily inorganic ions such as Na^+, K^+, Cl^- and small organic molecules such as amino acids and urea termed organic osmolytes. In terms of inorganic ions, regulatory volume decrease occurs by the loss of K^+/Cl^- *via* activation of K^+ and Cl^- channels or by activation of the K^+-Cl^- cotransporter (Chamberlin and Strange, 1989). Regulatory volume increase occurs by both an uptake of K^+/Cl^- and Na^+/Cl^- *via* activation of the Na^+- K^+-ATPase, Na^+/H^+ exchangers, Cl^-/HCO_3^- exchangers, Na^+ and Cl^- channels or Na^+-K^+-$2Cl^-$ cotransporters (Fig. 1). In addition to inorganic ions, organic osmolytes such as polyols, amino acids, and methylamines play key roles in cell volume homeostasis where they are released from the cell drawing water along with them to reduce swelling (Henry, 1995; Junankar and Kirk, 2000). Organic osmolytes have the ability to accumulate from tens to hundreds of millimolar concentrations without triggering detrimental effects on cellular structure and function (Yancey, 2001). Accumulation of these organic osmolytes occurs through energy-dependent transport, amino acid transporters, or changes in the rates of osmolyte synthesis/degradation (Gilles and Péqueux, 1981; Henry, 1995). The loss of organic osmolytes is triggered by cell swelling which causes efflux and downregulation of the synthesis of organic osmolytes (Junankar and Kirk, 2000).

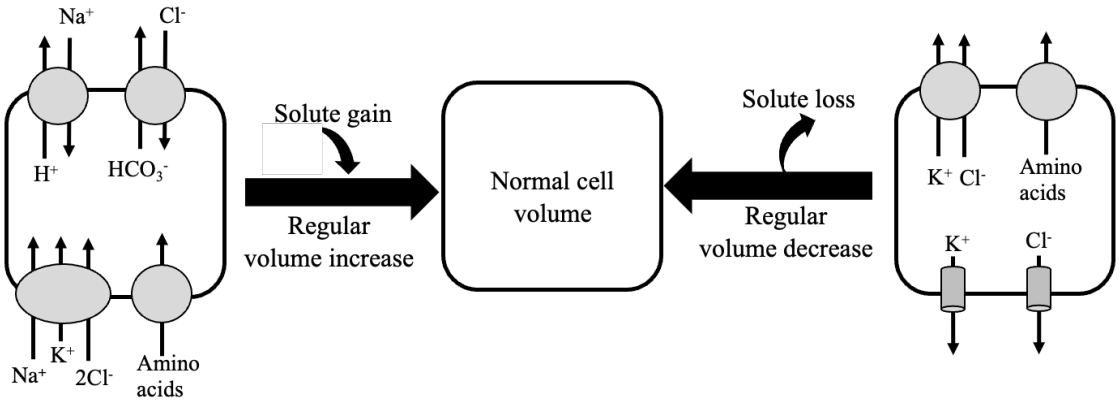

Figure 1: Schematic representation of transporters and processes involved in regulatory cell volume increase and decrease.

In addition to the movement of osmolytes, the movement of water across cells also contributes to cell volume regulatory processes. There are three ways in which the movement of water through cells and epithelia can occur: transcellular diffusion, paracellular diffusion, and facilitated diffusion through water channels referred to as aquaporins (AQPs). All three pathways of water movement are a result of osmotic gradients established by the transport of ions (Fig. 2). Transcellular and paracellular diffusion of water is the unfacilitated movement of water across the plasma membrane or intercellular/tight junctions, respectively, due to an osmotic gradient existing between the cell and its extracellular fluid (Komarova and Malik, 2010). These unfacilitated means of diffusion occur relatively slowly due to the polar properties of water and the hydrophobic core of phospholipid bilayers (Agre and Kozono, 2003). Aquaporins are part of the membrane integral proteins (MIPs) family and function as channels and are typically regulators of intracellular and intercellular water flux allowing its diffusion to occur much faster than transcellular or paracellular diffusion (Agre, 2004).

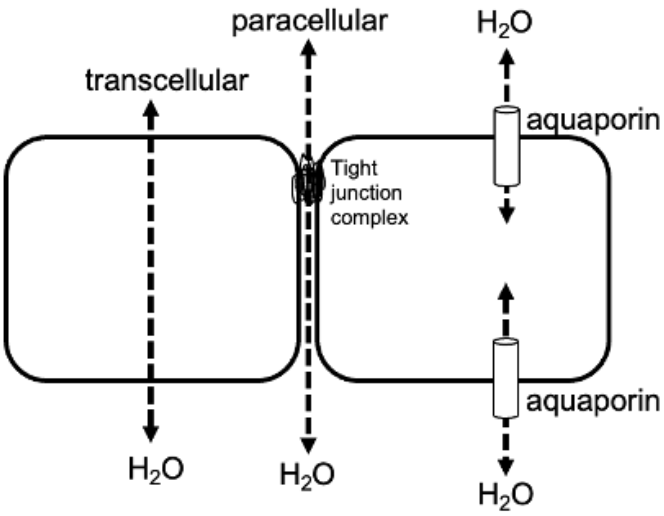

Figure 2: Possible pathways for transepithelial water movement. Water crosses the epithelial cell barrier through paracellular and transcellular pathways *via* unfacilitated diffusion through lipid bilayers, or by facilitated diffusion through aquaporins water channels. All pathways of water transport occur down an osmotic pressure gradient.

1.2 Structure of AQPs

Aquaporins are a family of transmembrane channel proteins that typically facilitate the transcellular flow of water across membranes in response to changes in osmotic and/or hydrostatic pressure. Although AQPs are widely distributed throughout all kingdoms of life, their overall structure is largely conserved (Fig. 3). Aquaporins are tetrameric proteins composed of monomers that each function as independent water channels. Each monomer has six transmembrane helices connected by five loops (named A–E), with the hydrophilic terminal amino and carboxyl groups located in the cell cytoplasm (Agre et al., 1993). Loops B and E contain highly conserved asparagine-proline-alanine (NPA) motif sequences (Fig. 3) which are stabilized through ion pairs and hydrogen bonds with neighbouring transmembrane helices to create the central pore (Sui et al., 2001). The six transmembrane α-helices surround the single narrow channel creating an "hourglass" shape. The highly conserved aromatic/arginine (ar/R) constriction site acts as a selectivity filter for water or other small solutes (Benga, 2012). The central constriction of the channel is lined with hydrophobic amino acid residues and has a diameter of about 3 angstrom (Å) which is only slightly larger than the 2.8 Å diameter of the

water molecule. This allows only one water molecule to pass through the channel at a time (Tani et al., 2009). Single water molecules enter the pore with the oxygen atom entering first. At some point, the water molecule reverses the orientation with the hydrogen atoms now pointing downwards. This molecular dynamic is controlled by the electrical field formed by the amino acid residues of the channel of the aquaporin (Murata et al., 2000). Aquaporins that allow small solutes or gases other than water have a larger pore opening, which can reach ~3.4 Å in diameter (Sales et al., 2013).

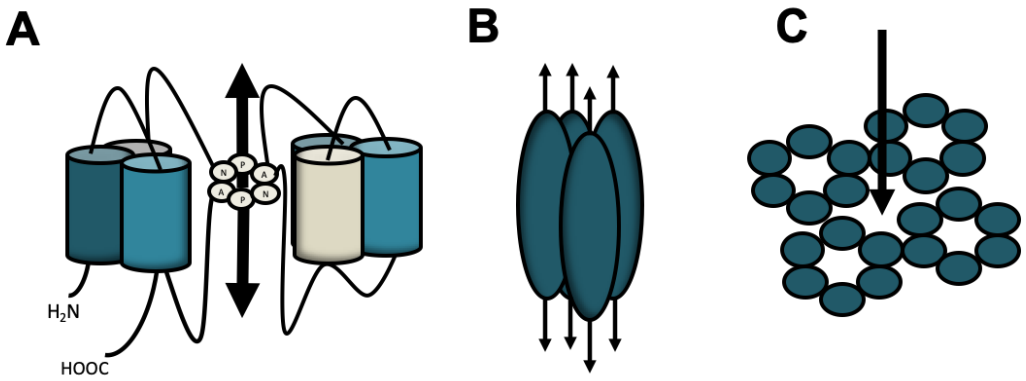

Figure 3*:* Schematic representation of aquaporin structure. (A) The structure of an individual aquaporin monomer containing six α-helices connected by three extracellular and two intracellular loops. The route of water passage exists in the transmembrane pore formed by the NPA motifs interacting within the membrane. (B) AQP monomers form a homotetramer to create four pathways for solute transfer while (C) the central pore of the tetramer may also form a fifth pathway.

1.3 AQPs in Terrestrial Vertebrates-Mammals

It had long been predicted that water movement across cell membranes was facilitated by pores or channels; however, it was not until the late 1980s that the first AQP was discovered. Although there is some debate as to who was the first to discover the AQP protein, Peter Agre was awarded the Nobel Prize in Chemistry in 2003 for this discovery (Agre, 2004; Agre et al., 1993; Benga, 1988; Benga et al., 1986; Denker et al., 1988; Preston et al., 1992). The discovery of the first water channel occurred when Agre and colleagues detected a highly abundant 28 kDa protein in red blood cell membranes that copurified with but was immunologically distinct from, the Rhesus antigen (Denker et al., 1988). The defining moment came when the Agre group injected mRNA encoding this 28 kDa protein into an expression system, *Xenopus laevis* oocytes,

and exposed them to distilled water. The mRNA injected into the oocytes resulted in the synthesis and expression of a new protein that caused the membrane to become highly permeable to water. A series of subsequent papers confirmed that this new protein, initially called CHIP28 (channel-forming integral membrane protein of 28 kDa) and later renamed aquaporin-1, was the first water channel to be definitively identified (Agre, 2004; Preston et al., 1992).

Currently, 13 mammalian AQP isoforms have been identified, extensively studied, and further classified into subfamilies based on their structural and substrate similarities. Classical aquaporins (AQP0, AQP1, AQP2, AQP4, AQP5, AQP6) are classified as those that have high water permeability capabilities. Aquaporins known to transport small uncharged compounds such as glycerol or urea in addition to water are classified as aquaglyceroporins (AQP3, AQP7, AQP9, AQP10) while aquaamoniaporins have been shown to transport ammonia (AQP8; Finn and Cerdà, 2015). Recently, an additional group known as the unorthodox aquaporins (AQP11 and AQP12) was discovered whose structure is different from that of other aquaporin groups, specifically concerning the generally conserved NPA motifs; however, virtually no additional characteristics have been defined for this group (Rojek et al., 2008; Yang, 2017).

Differential expression and the cellular localization of aquaporin isoforms within tissues play an important role in determining their physiological functions, especially in tissues involved in osmoregulation. The mammalian kidney is one of the most extensively studied systems that regulate systemic water balance. Different regions of the kidney's nephrons have distinct water permeabilities that correlate with the presence or absence of aquaporins (Li et al., 2017). Within the human kidney, nine aquaporins (AQP1-8, AQP11) are differentially expressed along the renal tubules and collecting ducts (Fig. 4) where they play crucial roles in the regulation of water homeostasis and urine concentration (Su et al., 2020). Aquaporin-1 is highly expressed in both the apical and basolateral membranes of the proximal tubules, the thin descending loop of Henle, and the endothelial cells of descending vasa recta. The main function of AQP1 is to absorb the bulk of water in the filtrate as ions are reabsorbed into the blood, accounting for up to 70% of the total water reabsorption (Su et al., 2020). Isoforms AQP2-6 are localized within the collecting duct. The AQP2–4 isoforms are exclusively expressed in the principal cells of the connecting tubules and collecting ducts. Isoforms AQP2 and AQP3 are under tight regulation by the antidiuretic hormone arginine vasopressin which can rapidly translocate these AQPs from their

intracellular storage vesicles to the apical membrane, permitting the tissue to modify its water permeability as required (Su et al., 2020). Aquaporin-3 has a reduced transporting water capability; however, it functions as an efficient transporter of glycerol in the basolateral membrane of the collecting duct to concentrate urine. Aquaporin-4 is also expressed in the basolateral membrane of the collecting duct and its main function is to further enhance water reabsorption (Chou et al., 1998). Aquaporin-5 is barely detectable through mRNA expression analyses or immunoblot assays, but it has been located in the apical membrane of the renal cortex (Procino et al., 2011). Aquaporin-6 is localized in intracellular vesicles with H^+-ATPase in renal collecting ducts and although has relatively low water permeability is capable of transporting anions (NO_3^-). The unique anion permeability by AQP6 activated at low pH supports the possible role in acid secretion (Yasui et al., 1999). Similar to AQP3, AQP7 shows a limited involvement in renal water reabsorption but plays a critical role in glycerol reabsorption in the brush border of the proximal tubule (Sohara et al., 2005). The AQP8 isoform is expressed in low levels within the proximal tubules, collecting duct, and in the inner mitochondrial membrane of renal proximal cells where it is thought to be important in mitochondrial ammonia transport; however, the full functions of AQP7 and AQP8 have yet to be identified (Su et al., 2020). The unorthodox AQP11 is regulated by glucose in the proximal tubules and is thought to be involved in osmoregulation within the endoplasmic reticulum (Su et al., 2020).

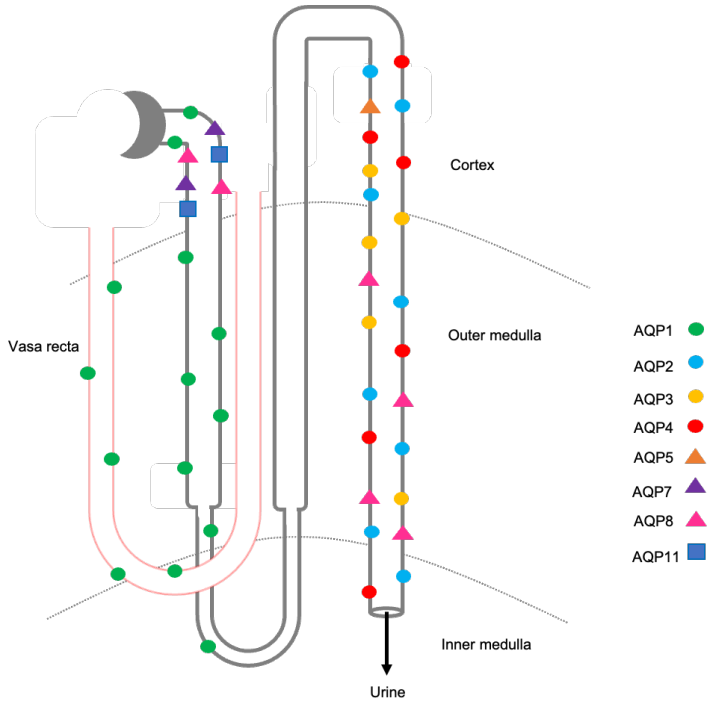

Figure 4: Intrarenal expression profile of aquaporins (AQPs) in the mammalian kidneys. The figure is a modification of that presented by Su et al. (2020).

1.4 AQPs in Aquatic Vertebrates-Fish

In teleost fish, osmotic balance is regulated by ion and water transport processes by three main osmoregulatory organs: the gills, gastrointestinal tract, and kidneys. Seawater teleost fishes maintain their extracellular fluids at an osmolality below that of their ambient environment creating an osmotic gradient that promotes the loss of body water and influx of environmental solutes. These fishes counteract the osmotic loss of water to the hyperosmotic environment by drinking seawater and reducing their rate of glomerular filtration and urine production. The diffusive movement of ions into the bodily fluids experienced by seawater fish is compensated by the active secretion of Na^+ and Cl^- across their gills (Larsen et al., 2014). In contrast, freshwater teleost fishes maintain their extracellular fluids at an osmolality above that of their ambient environment causing them to continuously gain body water and lose ions to the hypoosmotic environment. This problem is counteracted by producing large volumes of dilute urine and retaining ions *via* reabsorptive processes in the kidneys, the uptake of ions from food sources, and active Na^+/Cl^- uptake across the gills (Larsen et al., 2014). Euryhaline fish species

are capable of inhabiting both concentrated and dilute environments by shifting between these two osmoregulatory strategies depending on the osmolality of their immediate environment.

Although AQPs have been identified in a variety of teleost species their physiological role is overall poorly understood (Cerdà and Finn, 2010). The Atlantic salmon, *Salmo salar,* is often used as a euryhaline model species and has been used to study the role of AQPs in osmoregulation. Six AQP isoforms have been found in the *S. salar* transcriptome. Notably, AQP3 is found to be prominently expressed in the gill, AQP8 has high expression in the intestine, and AQP1b is predominantly expressed in the kidneys (Tipsmark et al., 2010). Transfer from freshwater to seawater induces a change in AQPs mRNA expression in gill, intestinal, and renal tissues which may have functional significance in the osmoregulatory capabilities of *S. salar* (Tipsmark et al., 2010).

The brachial mRNA expression of *S. salar* AQP1a and AQP3 decreased whereas AQP1b increased upon seawater acclimation. While their direct contact with the environment and blood is beneficial for the gills of fish to perform osmoregulatory ion fluxes, it also makes the epithelia a major site for water exchange. When maintaining extracellular fluid osmolalities above that of the immediate environment, it would be beneficial to keep transepithelial water permeability to a minimum; however, this is not always possible (Hill et al., 2004). Brachial cells must therefore have a high capacity for regulatory volume adjustments depending on the external environment's osmolality and could be partially accomplished by having low apical water permeability and high basolateral water permeability. The response of branchial AQPs mRNA expression to salinity challenges in *S. salar* may correspond to cellular reorganization occurring during salinity shifts (Tipsmark et al., 2010).

Both intestinal AQP1a and AQP1b mRNA levels increased in seawater acclimated *S. salar* but expression levels were higher in the muscle than in the enterocytes, which seem to suggest a minor role in enterocyte water transport (Tipsmark et al., 2010). The AQP1a may be localized in and facilitate water transport across endothelial cells, which was found to be a major site of AQP expression in the intestine of eels (Martinez et al., 2005). The isoform AQP8b was almost exclusively expressed in the mucosal layer of intestinal segments of *S. salar* and showed a substantial increase after seawater exposure. In addition, AQP8b was the only isoform predominantly expressed in the intestine, which suggests a particular significance in water uptake in seawater (Tipsmark et al., 2010).

Unlike mammalian kidneys, teleost kidneys are not capable of producing hyperosmotic urine (Stanley and Fleming, 1964). Although, isosmotic conditions may be reached in the urine of euryhaline fish during acclimation to hypersaline conditions by increasing the rate of water reabsorption from the glomerular filtrate within the distal segments of the nephrons. Aquaporin-1a mRNA expression was greatly elevated after the seawater transfer which is thought to increase renal water reabsorption (Tipsmark et al., 2010). Both AQP3 and AQP10 mRNA expression was also elevated during seawater acclimation suggesting these isoforms are additionally involved in renal fluid balance and water reabsorption in seawater salmon (Tipsmark et al., 2010).

Investigations of the role of AQPs in fishes are only just beginning and further investigations are still needed including measurements of protein expression changes, cellular localization patterns, and functional expression analyses of the isoforms in a variety of species to further understand their osmoregulatory role in teleost fishes.

1.5 Invertebrate AQPs- Insects

Aquaporins have been well characterized in vertebrate classes, but to a lesser extent in invertebrate classes. Most invertebrate AQP studies have primarily focused on insect model species, namely *Drosophila melanogaster* and *Aedes aegypti*. In insects, an alternative nomenclature system is typically used that characterizes AQPs by their phylogeny and function. These subfamilies include the DRIPs, PRIPs, and BIBs. The DRIP family, named after the *Drosophila melanogaster* gene, DRIP (DmDRIP), is most similar to the mammalian water selective AQP4 isoform. The *D. melanogaster* DRIP has been functionally expressed in *Xenopus* oocytes and acts as a water-specific AQP (Kaufmann et al., 2005). The second subfamily, the PRIPs, named after the firefly, *Pyrocoelia rufa*, have been functionally characterized as water-specific AQPs, similar to the DRIP family (Kikawada et al., 2008). The third subfamily of insect AQPs is the *D. melanogaster* Big Brain (DmBIB) proteins. The *D. melanogaster* Big Brain protein has been characterized not as a water channel but as a non-selective cation channel when expressed in *Xenopus* oocytes and is thought to be regulated by tyrosine-kinase activity (Yanochko and Yool, 2002). Through mutagenesis experiments, DmBIB has also been determined to play a role in determining neural fate (Doherty et al., 1997).

The Malpighian tubules have long been used as models for investigations into the mechanisms of fluid and ion transport in insects. Malpighian tubules are excretory organs composed of a single cell layer of blind-ended tubules that lie within the abdominal body cavity and empty into the junction between midgut and hindgut (Maddrell, 1964). Malpighian tubules function similarly to the vertebrate kidneys that contain AQP channels and transporters that facilitate the transport of water and other solutes across the basal and apical membrane of their cells (Drake et al., 2015). For example, in the yellow fever mosquito, *A. aegypti,* AQPs 1, 2, 4 and 5 have been confirmed to be expressed in the Malpighian tubules where they function as water channels and mediate transcellular water and solute transport in adult females (Drake et al., 2015). Female yellow fever mosquitos require an uptake of vertebrate blood for reproduction. During blood meals, mosquitoes start to produce large amounts of urine to eliminate excess body water while absorbing nutrients. Excess water is secreted from the Malpighian tubules into the lumen of the gut where it is excreted through the hindgut and rectum (Drake et al., 2015). The *A. aegypti* AQP1is localized in the tracheolar cells that are associated with the Malpighian tubules and functions as a water channel when expressed heterologously in *Xenopus* oocytes (Drake et al., 2015). Similarly, *A. aegypti* AQP2 and AQP5 showed high water transport capabilities when expressed in *Xenopus* oocytes. In addition to water transport, when expressed in *Xenopus* oocytes, *A. aegypti* AQP4 was also found to significantly enhance the uptake of glycerol, urea, erythritol, adonitol, mannitol, and trehalose (Drake et al., 2015). These findings support that AQPs expressed in the Malpighian tubules are involved in the regulation of adult female mosquito water homeostasis and solute reabsorption.

The larvae of *A. aegypti* are primarily found in freshwater and keep their internal body fluids hyperosmotic to the environment and thus face an influx of water due to the osmotic gradient. Under these conditions, an organ called the anal papillae function to actively absorb ions from the external environment, across the epithelium and into the hemolymph (Akhter et al., 2017). The anal papillae are composed of a thin epithelium covered by a cuticle and in addition to the Malpighian tubules are in part responsible for osmoregulatory functions in larval *A. aegypti*. Aquaporins expressed in the anal papillae of larval *A. aegypti* are sites of water permeability and greatly exaggerate the influx of water from their dilute environment (Akhter et al., 2017). Water uptake *via* AQPs by the anal papillae would seem counterproductive and the physiological basis for the observed expression of AQPs in larvae inhabiting dilute conditions is

not understood fully. The mRNA of six AQPs (AQP1-6) are found to be expressed within the anal papillae of larval *A. aegypti* where AQP4 and AQP5 are localized to the syncytial epithelium of the anal papillae (Akhter et al., 2017). It has also been shown that when larval *A. aegypti* are exposed to brackish conditions, AQP5 expression increases (Akhter et al., 2017). Further investigation is still needed to understand the role of AQPs of *A. aegypti* in dilute conditions; however, AQPs do seem to play a role in osmoregulation while in brackish conditions.

1.6 Invertebrate AQPs- Crustaceans

While literature concerning osmoregulation in invertebrates exists, few studies have characterized or investigated the importance of AQPs in these animals despite their likeliness to experience osmotic stress (Henry et al., 2012). Euryhaline and coastal invertebrates face regular osmotic challenges due to migration, inhabitation of tide pools, tidal action, or air exposure/semi-terrestrialism (Larsen et al., 2014). These lifestyles expose crustaceans to major osmotic challenges resulting in transepithelial water fluxes across their outer epithelia, especially across respiratory surfaces whose cuticle is not calcified (Rivera-Ingraham and Lignot, 2017). This water flux is threatening to the bodily fluids of aquatic crustaceans and therefore must be regulated.

While the transepithelial movement of Na^+ and Cl^- provide an osmotic driving force that promotes the movement of water through paracellular pathways, the presence of AQPs can greatly increase the rate of water flux by facilitating its transmembrane movement (Larsen et al., 2014). Crustaceans may change the water permeability of their tissues in response to fluctuating salinity as part of their osmoregulatory mechanism (Rahi et al., 2018). Evidence for this has been found in the Japanese blue crab, *Portunus trituberculatus,* where a transcriptomic analysis revealed that branchial AQP1 mRNA expression decreased in response to long-term hypo- and hyper-osmotic stress (Lv et al., 2013). Reducing the mRNA expression levels of branchial AQPs may operate as a protective mechanism to reduce the shrinking and swelling of cells within the gill (Lv et al., 2013). Similar findings were also found in the bay barnacle, *Balanus improvisus*, whose mantle AQP1 mRNA expression decreased by 121-fold when transferred from seawater to 3 ppt. water for 2 weeks (Lind et al., 2017). In contrast, the gills of the whiteleg shrimp,

Litopenaeus vannamei, increased the mRNA expression of an AQP by 113-fold when transferred from 20 to 3 ppt. for 24 hours (Wang et al., 2015). Similar results were also identified in larval *Callinectes sapidus* where an AQP1-like paralog's mRNA expression levels increased following a 96-hour exposure to 15 from 30 ppt. salinity (Chung et al., 2012).

In addition to altering the capacity for transcellular water movement, isoforms of the aquaglyceroporin (GLP) subfamily have also been shown to allow the transport of small ions in crustaceans. In the salmon louse, *Lepeophtheirus salmonis,* GLP1 version 1, GLP2, GLP3 version and GLP3 version 2 were each found to transport water, glycerol, and urea (Stavang et al., 2015). Aquaglyceroporins were also found in the bay barnacle, *B. improvises* where the GLP2 isoform was also found to transport water and glycerol (Lind et al., 2017). Although these functional analyses are important, the physiological importance of crustacean aquaglyceroporins which would include their sub-cellular localization and induction has not been determined.

Members of the big brain proteins (BIBs) subfamily have also been identified in *L. salmonis*, and *B. improvises* (Lind et al., 2017; Stavang et al., 2015). Heterologous expression of the *L. salmonis* BIB channel in *X. laevis* oocytes did not alter the oocyte's water permeability compared to controls. The lack of water transport of *L. salmonis* BIB is thought to be a result of an unusual constriction residue at the entrance to the pore and may support a role of ion transport and/or cell adhesion as reported for the *Drosophila* BIB (Stavang et al., 2015; Yanochko and Yool, 2002).

1.7 Mechanisms of Osmoregulation in Carcinus maenas

The green shore crab, *Carcinus maenas*, is a euryhaline weak osmoregulating crab tolerant of salinities between 10-35 ppt (Henry, 2005; Henry et al., 2012; Nagel, 1934). Although *C. maenas* is native to the Atlantic and Baltic coasts of Europe it is one of the most successful global invaders having colonized the coasts of North and South America, Australia, Southern Africa, and Japan (Compton et al., 2010; Grosholz and Ruiz, 1996). A major factor in its success as an invader relates to its ability to permanently inhabit fully marine and dilute environments (Larsen et al., 2014; Rathmayer and Siebers, 2001; Siebers et al., 1983; Winkler et al., 1988), temporarily reside within tide-pools (Truchot, 1988), and undergo short-term emersion (Rivera-Ingraham and Lignot, 2017; Simonik and Henry, 2014). *Carcinus'* tolerance to osmotic stress

stems from its ability to shift from an osmoconforming state in seawater to an osmoregulatory in dilute media below 26 ppt. (Henry, 2005; Kirschner, 2004). This phenomenon is achieved through the active uptake of environmental Na^+ and Cl^- across the crab's posterior gills (pairs #7-9; Siebers et al., 1982). In dilute salinities, the posterior gills of *Carcinus* undergo morphological changes that increase the number of basolateral infoldings and the abundance of mitochondria to support the active uptake of environmental Na^+ and Cl^- (Compere et al., 1989; Copeland and Fitzjarrell, 1968; Freire et al., 2008; Neufeld et al., 1980). The main driving force for the active uptake of Na^+ and Cl^- from the environment across the posterior gills of *C. maenas* (Fig. 5) is the active (*i.e.* ATP-dependent) export of three cytosolic Na^+ into the hemolymph and importation of two K^+ from the hemolymph into the cytosol across the basolateral membrane by the Na^+/K^+-ATPase that keeps cytosolic [Na^+] low and hyperpolarizes the epithelia (Lucu and Siebers, 1987; Siebers et al., 1985). Basolateral K^+ channels allow cytosolic K^+ to flow back into the hemolymph, essentially allowing the ions to be recycled for use by the Na^+/K^+-ATPase (Onken et al., 1991; Riestenpatt et al., 1996). Due to the electrochemical gradients established by the Na^+/K^+-ATPase, Na^+ within the environment is drawn toward the epithelia and can enter the hemolymph directly *via* paracellular diffusion or through apical transporters including the $Na^+/K^+/2Cl^-$ cotransporter (Riestenpatt et al., 1996; Towle and Weihrauch, 2001) whose activity is dependent on K^+-recycling achieved through apically expressed K^+ channels (Lucu and Towle, 2010; Onken et al., 2003; Riestenpatt et al., 1996). Chloride ions crossing the apical membrane through $Na^+/K^+/2Cl^-$ cotransporter activity are moved into the hemolymph across basolateral Cl^- channels due to the electronegativity of the cytosol relative to the hemolymph (Lucu and Siebers, 1987; Onken et al., 1991; Riestenpatt et al., 1996). Apical Na^+/H^+ and Cl^-/HCO_3^- exchangers also contribute to the absorption of Na^+/Cl^- from the environment, linking carbonic anhydrase to the osmoregulatory process due to its ability to catalytically hydrate intracellular CO_2 (either metabolically produced or sourced from the hemolymph through Rhesus-protein mediated diffusion into the cytosol; Endeward et al., 2008; Soupene et al., 2004; Thies et al., 2022) to form the counter-ions used by the exchangers (Henry, 2005, 2001; Henry et al., 2003; Lucu, 1989; Siebers et al., 1987). This mechanism (Fig. 5) allows *C. maenas* to maintain its extracellular osmolality well above that of its environment; however, it also creates an osmotic gradient that promotes an influx of water across the crab's body. The excess water may be eliminated from the animal through the production of hypoosmotic urine by the ultrafiltrating antennal glands,

although its mechanism is poorly understood (Henry, 1995; Tsai and Lin, 2014). These results may not represent all aquatic brachyuran equally; however, they should operate as a comparable model for other weak osmoregulators that do not depend on an apical V-type H+-ATPase (Henry et al., 2012).

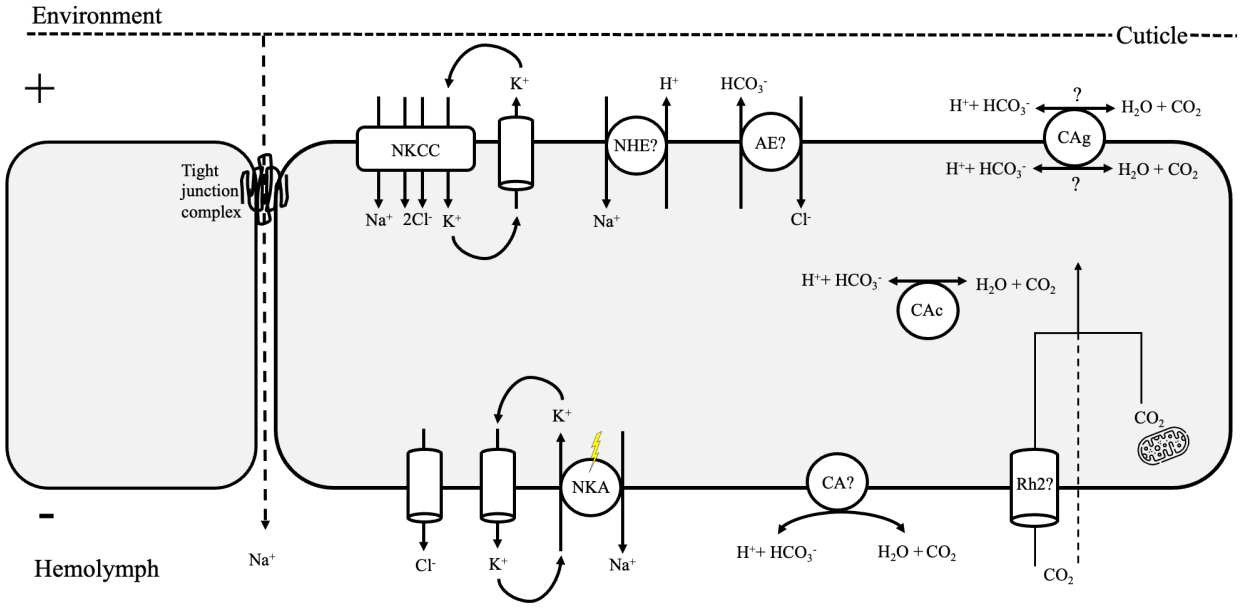

Figure 5: Hypothetical mechanism of transbranchial Na^+ and Cl^- absorption in osmoregulating *Carcinus maenas* based on the models presented for moderately leaky weak osmoregulators by Henry et al. (2012). Primary active transport is indicated by lightning bolts, question marks indicate a transporter, enzyme, or reaction whose specific identity and/or cellular localization are hypothesized but not determined.

1.8 The role of urea in osmoregulation in crustaceans

Although often viewed as an excretable form of nitrogenous waste, some species are known to use urea for osmoregulatory purposes. It has been well documented that within the mammalian kidneys, urea is used as a non-ionic osmolyte to adjust the osmolality of urine and the amount of water being excreted during diuretic and antidiuretic regulatory processes (Fenton, 2009; Higgins, 2016). In brief, the process involves the concentration of urea within the collecting duct to create an osmotic gradient promoting the aquaporin-facilitated movement of water across the epithelia into the blood. Hormones such as vasopressin, also known as the anti-diuresis hormone (ADH), signal for the insertion of more aquaporins into the collecting duct

epithelia and the insertion of urea transporters at the duct's distal region to recycle urea from the duct, through the medulla, and into the ascending limb to greatly enhance water reabsorption (Fenton, 2009; Higgins, 2016).

Despite its prevalence in mammalian osmoregulation, the putative osmoregulatory role of urea in osmoregulating crustaceans has not been considered. Aquatic crustaceans are ammonotelic with urea excretion only accounting for 20% of the total nitrogen excreted in freshwater and seawater species (Delaunay, 1931; Dresel and Moyle, 1950; Jawed, 1969; Krishnamoorthy and Srihari, 1973; Needham, 1957; Weihrauch et al., 1999a). However, in *C. maenas*, hemolymph urea concentrations increase during acclimation to dilute salinity from ca. 20–80 μmol l^{-1} in seawater-acclimated crabs to 600–1000 μmol l^{-1} in crabs acclimated to 10 ppt. salinity. Additionally, when the gills of brackish acclimated *C. maenas* were perfused employing an outwardly directed urea gradient of 600:0 μmol l^{-1}, no branchial urea excretion was found indicating the gills were not permeable for urea (Weihrauch et al., 2009, 1999b). In fact, the gills appeared to increase their energetic expense during this perfusion, as suggested by a 71% increase in branchial metabolic ammonia production, providing some indication that an energy consuming urea retention mechanism may exist (Weihrauch et al., 2009, 1999b). Given that hemolymph urea has not been given a conclusive physiological significance in aquatic crustaceans, the elevation of hemolymph urea under dilute conditions may indicate an osmoregulatory potential.

1.9 Carcinus maenas aquaporins

This thesis employs the well-characterized euryhaline green shore crab, *Carcinus maenas*, as an experimental osmoregulatory model. For decades, research has focused on Na^+ and Cl^- movements across their multifunctional gills; however, the importance of water flux has been untouched despite the changing osmotic pressure gradients associated with the osmoregulatory activity. Presented here is the investigated potential osmoregulatory role of AQP-mediated water and urea transport in aquatic brachyurans. Putative AQP isoforms were identified in a transcriptome of *C. maenas* and classified based on their structural homology to AQPs of other known AQP sequences. Heterologous expression of *C. maenas'* AQP isoforms in *Xenopus laevis* oocytes determined their water and urea transport capabilities. Differences in the

mRNA expression of the AQPs were measured in long-term seawater and brackish water acclimated *C. maenas*. Furthermore, changes in the AQP isoform's mRNA expression levels were measured in parallel to changes in the hemolymph and urinary osmolality of seawater-acclimated *C. maenas* upon acute hypoosmotic stress.

1.8 Aims and Objectives

This thesis aims to identify and characterize aquaporins (AQPs) in the euryhaline model species, *Carcinus maenas* and investigate their potential osmoregulatory role.

The objectives of this study include:

1. To screen the transcriptome of *C. maenas* to obtain sequence information of potential AQPs.

2. Use the Maximum Likelihood sequence analysis method to classify potential *C. maenas* AQPs into subfamilies of AQPs to identify predicted substrates.

3. Use quantitative PCR (qPCR) to determine tissue and salinity-specific gene expression of *C. maenas* AQPs.

4. Determine cellular localization of *C. maenas* classical AQP (CmAQP1) to investigate the potential role of CmAQP1 in osmoregulation and cell volume regulation in brachial tissue.

5. Use qPCR to determine mRNA response of identified AQPs to acute salinity stress in osmoregulatory tissues: the gills and the antennal gland.

6. Investigate *C. maenas'* hemolymph and urine osmolality during exposure to brackish conditions for 7 days to identify the potential role of AQPs in water permeability across body surfaces in dilute conditions.

7. Examine the urea content in *C. maenas'* hemolymph and urine during exposure to brackish conditions for 7 days to investigate the use of urea as an osmolyte.

8. Functionally express *C. maenas* AQP1, GLP1 and, BIB1 in the expression system of *Xenopus laevis* oocytes, to determine substrates of these isoforms by measurement of the oocyte osmotic water permeability in hypoosmotic stress and radioactive urea uptake.

1.9 Hypotheses

1. The mRNA abundance of *C. maenas* AQP1, GLP1, and BIB1 transcripts will be lower in *C. maenas* gills, antennal glands, hindgut, ganglia, and claw muscle tissues acclimated to brackish water conditions (10 ppt) compared to in seawater conditions (32 ppt.).

2. Low salinity exposure (10 ppt.) of 2 and 7 days will result in a decrease in mRNA expression of *C. maeans* AQPs in osmoregulatory tissues, gills, and antennal glands.

3. Urine osmolality will decrease when in brackish water to produce hypoosmotic urine.

4. Hemolymph urea concentration will increase during exposure to brackish conditions.

5. Functional expression of *C. maenas* AQPs will reveal the substrate(s) will be largely conserved to their predicted orthologs subfamilies.

2.0 Materials and Methods

2.1 Animals

Wild-caught adult male *C. maenas* were obtained from Northern Placentia Bay, Newfoundland, Canada, located in the North Atlantic Ocean and subsequently transported to the Animal Holding Facility at the University of Manitoba (Winnipeg, Manitoba, Canada). Prior to experimentation, animals were maintained in either 1200-gallons of recirculating artificial seawater (32 ppt., pH 8.1, 14ºC; Fritz Reef Pro Mix (RPM), Fritz Aquatics, Mesquite, TX, USA) or recirculating 300-gallon tanks of brackish water (10 ppt., pH 8.1, 14ºC, Fritz RPM). The light: dark cycle was kept to 14:10 hours for both conditions. The shelter was provided in the form of PVC pipes and plastic structures. Crabs were fed an ad libitum diet of bay scallops every 3 days. Experimental animals were fasted for 3-days prior to experimentation to reduce the effects of feeding on collected data.

2.2 Hypoosmotic stress and fluid collection

Prior to experimentation, seawater-acclimated crabs were transferred from their general housing aquaria to a recirculating 60-gallon tank of continuously aerated seawater (32 ppt., pH 8.1, Fritz RPM) whose 14ºC temperature and 14:10 hour light: dark cycle were maintained by a controlled environmental room (Conviron, Winnipeg, MB, CA). Individuals were identified by symbolic markings painted on their exoskeleton with nail polish. After a week of acclimation to the 32 ppt. experimental setup, hemolymph and urine samples were collected (t = 0 h) and the environmental salinity was subsequently reduced directly to 10 ppt. Hemolymph (*ca*. 150 µl) was sampled from the arthrodial membrane of the rear walking leg using an 18-gauge needle whereas urine was aspirated from the deflected nephropore using a pipet after thoroughly drying the crab's anterior region as described by Allen et al. (2021). Additional hemolymph and urine samples were collected after 3, 6, 12,18, 24, 48, and 168 hours (7-days) of exposure to brackish conditions (10 ppt.). This exposure was repeated 3 times throughout this study, each using different groups of animals to reduce the effects of repeatedly sampling bodily fluids of the same individuals over a short period of time.

2.3 Osmolality measurements

Hemolymph, urine, and water samples collected from the first group of crabs (n = 8) exposed to hypoosmotic stress were immediately frozen at -20ºC until measurements were made within the following 48 hours. Osmolality was measured using a vapour pressure osmometer (VAPRO Model 5520, Wescor, UT, USA) calibrated to 100, 290, and 1000 mOsmol kg^{-1} commercial standards (Thermo Scientific).

2.4 Spectrophotometric measurement of urea

Previously frozen hemolymph and urine samples collected from the second group of animals exposed to hypoosmotic stress (n = 12) were deproteinized and neutralized prior to performing spectrophotometric measurements. Deproteinization was achieved by mixing samples with a 1:2 or 1:4 ratio of 6% perchloric acid prepared in an appropriate background of NaCl to match that of the sample. Acidified samples were then incubated on ice for 10-minutes prior to centrifugation (4ºC, 21,000 x *g*, 5 min). The supernatant was then collected and neutralized with 0.4 volumes of 3 mol l^{-1} KOH and centrifuged to remove the $KClO_4$ precipitate (4ºC, 21,000 x *g*, 5 min). This supernatant was then used to spectrophotometrically measure urea concentrations using a microplate adapted equivalent of the diacetyl monoxime/thiosemicarbazide method of Rahmatullah and Boyde (1980). In brief, 50 µl of deproteinized samples or equally treated urea standards were combined with an equal volume of urea assay reagent (containing 1.2 mol l^{-1} H_2SO_4, 0.33 mol l^{-1} H_3PO_4, 1.37 $\times 10^{-4}$ mol l^{-1} $FeCl_3$, 6.1 $\times 10^{-5}$ mol l^{-1} thiosemicarbazide, and 2.74 $\times 10^{-3}$ mol l^{-1} diacetyl monoxime) and subsequently incubated at 99ºC for 10 minutes. Samples were allowed to cool to room temperature prior to reading absorption measurements at a wavelength of 540 nm (Powerwave, BioTek, Winooski, VT, USA). To confirm that this assay was not detecting non-urea compounds, a 7-day in 10 ppt. hemolymph sample was measured in the presence and absence of urease (10 U ml^{-1}, 30 min at room temperature). The urease-treated sample had no detectable urea (data not shown).

2.5 Quantitative PCR

Crabs that were part of the third hypoosmotic stress experiment (n = 7) were placed on ice for 20-30 minutes and gill 5, gill 8, and antennal glands were dissected under RNase-free conditions and stored in RNAlater (Applied Biosystems, Austin, TX, USA) and were kept at 4°C for 24 hours prior to storage at −80°C until RNA isolation. The same procedures were performed on crabs that were long-term acclimated to either 32 ppt. or 10 ppt. conditions for more than 3 months to assess long-term differences in the distribution of target genes in gills 5 and 8, the antennal glands, claw muscle, hindgut epithelial cells, and ganglia. Total RNA was isolated from tissues with TRI Reagent (Sigma-Aldrich, St. Louis, MO, USA). The quality and quantity of the RNA were monitored spectrophotometrically using a NanoDrop 2000c spectrophotometer (Thermo Scientific, Ottawa, ON, CA). Prior to the synthesis of cDNA, 0.8 µg of the isolated total RNA was treated with DNase I (Invitrogen, MA, USA) to remove any potential DNA contamination. The DNase treatment was verified to be successful by the failure to amplify transcripts encoding a ribosomal protein (primer pair RPL8 F1/R1; Table 1) *via* PCR. Complementary DNA (cDNA) was then synthesized from 0.8 µg DNase-I-treated RNA using an iScript cDNA synthesis kit (Bio-Rad, Mississauga, ON, CA). Successful cDNA synthesis was evaluated by the amplification of RPL8 transcripts *via* PCR (primer pair RPL8 F1/R1; Table 1). All PCR products were assessed by ethidium bromide-stained TAE agarose gel electrophoresis.

Primer pairs were designed to target putative aquaporins (CmAQP1, CmGLP1, and CmBIB1) identified from a publicly available *C. maenas* transcriptome. Additional primers were designed to target transcripts encoding the ribosomal protein L8 (RPL8) and elongation factor 1 alpha (EF1α) to be used as housekeeping reference genes (Table 1). PCR products of the predicted size were purified from excised agarose gel fragments (E.Z.N.A Gel Extraction Kit, Bio Tek, Winooski, VT, USA) and sequenced by the Centre for Applied Genomics (Toronto, ON, CA) to verify the product's sequence prior to performing quantitative PCR (qPCR).

The qPCR reaction mixture for one reaction contained 5 µl of SsoAdvanced Universal SYBR Green Supermix (Biorad, Mississauga, ON, CA), 0.25 µl of a stock 10 µmol l^{-1} sense and antisense gene-specific primers to the final reaction concentrations of 250 nmol l^{-1} (Integrated DNA Technologies, IA, USA), 0.5 µl of molecular grade water and 4 µl of the template. The thermal cycle protocol (Biorad CFX connect) consisted of 3 minutes of initial denaturation at

98°C followed by 40 cycles with denaturing for 15 seconds at 98°C, annealing for 30 seconds and an elongation step for 30 seconds at 72°C. A melt curve analysis was used after thermal cycles to verify a single PCR product. The efficiency of the assay was assessed by the construction of standard curves. Standard curves were generated as a dilution series of cDNA where a minimum R2 value of 0.9 was required for all standard curves. Changes in the abundance of transcripts following 2 and 7-day hypoosmotic stress were normalized to CrabRPL8 or CmEF1α (F1/R1 primers; Table 1) using the Pfaffl (2004) method.

No housekeeping gene with constant mRNA expression levels could be identified for both 32 ppt. and 10 ppt. long-term acclimated green crabs across all tissues. Hence, absolute quantification was solely assessed using the included standard curve. In this case, a standard curve based on dilution of a corresponding purified PCR product was used (ten-fold serial dilution 1000 - 0.1 fg). Values are presented as copy numbers and were calculated using the following equation, where 6.02×10^{23} is Avogadro's Constant, the amount of DNA put into the reaction (ng) divided by the DNA template size (base pairs), 660 g mol^{-1} is the molecular weight of one base pair and 1×10^{9} ng (g^{-1}) is used to convert of molecular weight to ng:

$$\text{Copy number } (\text{ng}^{-1}) = \frac{6.02 \times 10^{23} \left(\text{copy mol}^{-1}\right) \times \text{DNA amount (ng)}}{\text{DNA template size (bp)} \times 660 \left(\text{g mol}^{-1}\right) \times 1 \times 10^{9} \text{ (ng g}^{-1})}$$

The CT values of the standard curves were plotted against the logarithm of their initial template copy numbers. The linear regression equation was then used to determine the logarithm copy number in each tissue. The resulting value was raised as an exponent to produce a copy number of each gene in each given tissue in long-term acclimated 32 ppt. and 10 ppt. crabs.

2.6 Obtaining the open reading frame of C. maenas aquaporins

Except for CmGLP1, full open reading frames (ORFs) sequences were previously published on Genbank (https://www.ncbi.nlm.nih.gov/genbank/). Degenerate primers (Table 2) were designed based on sequences of GLP-like of *Portunus trituberculatus* (GFFJ01052468.1) and *Eriocheir sinensis* (GFBL01038362.1) to amplify the missing 5' end of CmGLP1. Primers

were also designed on a published 3' end sequence for CmGLP1 (GBXE01131729.1) to amplify its 3' end (Table 2).

A cDNA template was used in obtaining CmGLP1 PCR products and was amplified using Q5 High-Fidelity DNA Polymerase (NEB, Whitby, ON, Canada) following this protocol: initial denaturation at 98°C for 3 minutes, followed by 45 cycles of: denaturation at 98°C 10 seconds, annealing at 50°C for 30 seconds, elongation at 72°C for 30 seconds and final elongation at 72°C for 2 minutes. Products were then excised and purified from agarose gels using the GeneJET Gel Extraction Kit (Thermo Scientific, Ottawa, ON, CA). The purified 5' and 3' end PCR products were then combined, re-amplified, and purified to produce the full ORF. The full CmGLP1 ORF was then subcloned into a pJET 1.2/blunt vector (Thermo Scientific) using DH5α *E.coli* competent cells (Invitrogen, Waltham, MA, USA). Bacterial colonies were purified using GeneJET Plasmid Miniprep Kit (Thermo Scientific, Ottawa, ON, CA) and sent for sequencing to confirm verify its sequence (Centre for Applied Genomics, Toronto, ON, CA) by comparing to the aforementioned GLP-like *P. trituberculatus* and *E. sinensis* nucleotide sequences.

Primer pairs were designed to target putative CmAQP1 identified from a publicly available *C. maenas* transcriptome (Table 3). The CmAQP1 ORF was amplified using a cDNA template and proofreading Phusion High-Fidelity DNA Polymerase (Thermo Scientific, Ottawa, ON, CA) using the following touchdown PCR protocol: initial denaturation at 98°C for 2 minutes, followed by 25 cycles of denaturation at 98°C for 20 seconds, annealing from 70-45°C for 15 seconds decreasing 1°C per cycle, elongation at 72°C for 1 minute, followed by 10 cycles of denaturation at 98°C for 20 seconds, annealing at 45°C for 15 seconds, elongation at 72°C 1 minute followed by a final elongation at 72°C for 10 minutes. The resultant CmAQP1 ORF gel fragment was extracted and purified using GeneJET Gel Extraction Kit (Thermo Scientific, Ottawa, ON, CA).

Primer pairs were designed to target putative CmBIB1 identified from a publicly available *C. maenas* transcriptome (Table 3). The CmBIB1 ORF was amplified from a cDNA template utilizing Q5 High-Fidelity DNA Polymerase (NEB, Whitby, ON, Canada). CmBIB1 was obtained using the following touchdown PCR protocol: initial denaturation at 98°C for 2 minutes followed by 20 cycles of denaturation at 98°C for 10 seconds, annealing from 70-50°C for 15 seconds decreasing 1°C per cycle, elongation at 72°C for 1 minute and 30 seconds,

followed by 15 cycles of denaturation at 98°C 10 seconds, annealing at 45°C for 15 seconds, elongation at 72°C for 1 minute and 30 seconds, followed by a final elongation at 72°C for 3 minutes. The CmBIB1 ORF gel fragment was extracted and purified using GeneJET Gel Extraction Kit (Thermo Scientific, Ottawa, ON, CA).

2.7 Cloning and sequence characterization of C. maenas aquaporins

To clone the full-length open reading frames the following procedures were performed: Primers containing restriction enzyme sequences (Table 2) were designed in the untranslated regions (UTRs) at the 5′ and 3′ ends to produce full-length clones that included the open reading frames (ORF). The purified ORF PCR products obtained in the previously mentioned section were used as a template utilizing Q5 High-Fidelity DNA Polymerase (NEB). The resulting full-length ORF PCR products were run on an agarose gel and purified with the GeneJET Gel Extraction Kit (Thermo Scientific). The purified ORF PCR products and custom-made *X. laevis* oocyte pGEM-HE vector were digested with corresponding restriction enzymes and ligated together with T4 ligase (Thermo Scientific). The custom-made pGEM-HE vector (Promega pGEM 3Z) contains 3' and 5' UTRs of a *Xenopus* beta-globin gene to be expressed in *Xenopus laevis* oocytes (Liman et al., 1992). The pGEM-HE vector containing the ligated aquaporin was cloned into DH5α *E. coli* cells (Invitrogen), and subsequent bacterial colonies produced were purified using GeneJET Plasmid Miniprep Kit (Thermo Scientific) and sequenced (Centre for Applied Genomics, Toronto, ON, CA). The sequence homology of CmAQP1, CmGLP1, and CmBIB1 were examined using the BLAST network server (blast.ncbi.nih.gov/Blast.cgi).

Once full-length open reading frames of CmAQP1, CmGLP1, and CmBIB1 were confirmed by sequencing, sequence analysis of the deduced amino acid sequences was performed. The deduced amino acid sequences of complete ORFs were used to predict the presence of transmembrane helices in the proteins using the TMHMM - 2.0 Prediction of transmembrane helices in proteins online tool (https://services.healthtech.dtu.dk/service.php?TMHMM-2.0). The CmBIB1 isoform was aligned with the *Drosophila melanogaster* BIB (for sequence reference see Table 3) to identify regions of transmembrane helices (TMH). Additionally, amino acid sequences were analyzed for the presence of signal peptides using SignalP 3.0 Server (http://www.cbs.dtu.dk/services/SignalP)

and the prediction of phosphorylation sites using NetPhos 2.0 Server with a minimum potential score of 0.9 was performed (http://www.cbs.dtu.dk/services/NetPhos/).

Sequence homology analyses were performed using the Maximum Likelihood method and Bayesian inference of the deduced amino acid alignments of non-redundant arthropod and human AQPs to create clusters of subfamilies. Orthologous sequences were obtained from open sources (Genbank, transcriptome shotgun assemblies, or sequences previously identified in published literature) and assembled using the COBALT Multiple Alignment Tool (https://www.ncbi.nlm.nih.gov/tools/cobalt/cobalt.cgi). Only full-length open reading frame sequences containing the two conserved NPA motif sites were included in the sequence analysis by the Maximum Likelihood method. A full list of the amino acid Genbank accession numbers of sequences used in the study is provided in Table 3. The sequence analysis by the Maximum Likelihood method and Bayesian interferences using the JTT matrix-based model was conducted in MEGA 11 (https://www.megasoftware.net) using a bootstrap analysis performed with 1000 replicates (Jones et al., 1992). The percentage of trees in which the associated taxa clustered together is shown next to the branches. Initial trees for the heuristic search were obtained automatically by applying Neighbor-Join and BioNJ algorithms to a matrix of pairwise distances estimated using the JTT model, then selecting the topology with a superior log-likelihood value. The tree is drawn to scale, with branch lengths measured in the number of substitutions per site. This analysis involved 61 amino acid sequences. There were a total of 1002 positions in the final dataset. Text formatting was adjusted in LibreOffice (https://www.libreoffice.org).

2.8 Capped RNA synthesis and expression of CmAQP1, CmGLP1, and CmBIB1 in Xenopus laevis oocytes

A single restriction digest of the pGEM-HE vector containing either CmAQP1, CmGLP1, or CmBIB1 was completed to synthesize capped mRNA (cRNA) by the HiScribe T7 ARCA mRNA kit (NEB). The restriction enzyme SPHI-HF (NEB) was used for CmAQP1 while NOTI (Thermo Scientific) was used for CmGLP1 and CmBIB1. Synthesized cRNA was DNase I treated and then purified using E.Z.N.A.® MicroElute RNA Clean-Up Kit (Omega Bio Tek, GA, USA). The cRNA was quantified spectrophotometrically (Nanodrop 2000c, Thermo Scientific) and the integrity was assessed on a MOPS agarose gel containing formaldehyde.

Oocytes were removed from mature female *Xenopus laevis* according to the approved animal protocol (#F20-021) and treated with collagenase type IV (Thermo Scientific), prepared in Ca^{2+}-free oocyte ringer (OR2; in mmol l^{-1}: 82.5 NaCl, 2.5 KCl, 1 $MgCl_2$, 1 Na_2HPO_4, 5 HEPES, pH 7.5), and gently agitated for 90 minutes at room temperature to free follicle cells. Collagenase activity was terminated by rinsing the oocytes three times in standard OR2 (containing 1 mmol l^{-1} $CaCl_2$). Oocytes at stages V and VI were selected for injections based on the presence of a distinct contrast between the black animal hemisphere and the white vegetal hemisphere (Newman et al., 2018). Selected oocytes were then rinsed four additional times with standard OR2 and allowed to recover in OR2 supplemented with 2.5 $mmol^{-1}$ sodium pyruvate, penicillin-streptomycin (1 mg ml^{-1}), and gentamicin (50 µg ml^{-1}) overnight at 17°C. The following day, individual oocytes were injected cytoplasmically with 36.0 ng $µl^{-1}$ of cRNA or nuclease-free water as a corresponding control using a Nanoject II auto-nanoliter injector (Drummond Scientific, PA, USA). Injected oocytes were rinsed twice daily with standard OR2 and incubated at 17°C with OR2 containing antibiotics and sodium pyruvate for 3 days until experimentation. All oocyte experiments were performed on two ovaries to confirm repeatability.

2.9 Water permeability assay

Injected oocytes were exposed to acute hypoosmotic stress to determine if the heterologously expressed *C. maenas* aquaporins transport water. Oocytes were initially exposed to an isosmotic OR2 (pH 7.5, osmolality 200 mOsmol kg^{-1}), and visualized under a microscope fitted with a video recorder (AmScope HDMI Model 1080P HD205-Wu Camera, PA, USA). The OR2 was then diluted to 37.5 mOsmol kg^{-1} to expose oocytes to hypoosmotic stress. Transport of water in cRNA-injected oocytes was quantified by the time required for the oocyte's membrane to rupture due to the hypoosmotic stress compared to control water-injected oocytes. The osmolality of the solutions was measured using a vapour pressure osmometer (VAPRO Model 5520, Wescor, UT, USA).

Due to their ability to transport water, oocytes expressing CmAQP1 and CmGLP1 were additionally bathed in standard OR2 containing a general AQP inhibitor ($NiCl_2$, 1 mmol l^{-1}) for 1

hour and then transferred to diluted OR2 (37.5 mOsmol kg^{-1}) containing 1 mmol l^{-1} $NiCl_2$ to determine if the observed transport of water of the oocyte was Ni^{2+} sensitive.

2.10 Urea uptake experiments

Two experiments were performed to identify whether any of the three AQP isoforms found within *Carcinus maenas* transport urea. Each experiment was repeated 3 times on two ovaries to confirm repeatability.

In the first experiment, groups of control (water-injected) or *C. maenas* aquaporins (cRNA- injected) oocytes (2 oocytes, 3 replicates; n = 6) were placed in 15-ml tubes and incubated at room temperature in OR2 solutions containing 1 mmol l^{-1} urea and radiolabeled urea (^{14}C-urea, 1 μCi ml^{-1}, Non-GLP grade, Moravek Inc, CA, USA) for either 10, 20, 30, or 60 minutes to optimize incubation period time (Fig. 14). Once the incubation period was complete, oocytes were rinsed three times with ice-cold standard OR2 containing 1 mmol l^{-1} urea. Individual oocytes were then lysed in 200 μl of 10% sodium dodecyl sulphate (SDS) and their radioactivity was quantified by scintillation counting using 3 ml Ultima-Gold scintillation cocktail (PerkinElmer, Waltham, MA, USA) in a Tri-Carb liquid scintillation counter (PerkinElmer) utilizing a 5-minute count protocol. In addition to the radioactivity of the oocytes, the radioactivity of the incubation and final washing buffer was also measured by adding 20 μl of the buffer to 3 ml Ultima-Gold scintillation cocktail (PerkinElmer). A 30-minute incubation period was selected for all following experiments.

In a second experiment, groups of control (water-injected) or CmGLP1 (cRNA- injected) oocytes (3 oocytes, 3 replicates; n = 9) were pre-incubated at room temperature in OR2 containing 1 mmol l^{-1} $NiCl_2$ for 1 hour to potentially inhibit CmGLP1 transport of urea. Once this incubation was complete, these oocytes were transferred to standard OR2 solution containing 1 mmol l^{-1} urea and its radiolabeled equivalent for 30 minutes (^{14}C-urea, 1 μCi ml^{-1}). Incubation was terminated by rinsing the oocytes three times with ice-cold standard OR2 containing 1 mmol l^{-1} urea and 1 mmol l^{-1} $NiCl_2$. Oocytes were then lysed in 200 μl of 10% SDS and their radioactivity was quantified by scintillation counting using 3 ml Ultima-Gold scintillation cocktail. The radioactivity of the incubation (40570 cpm) and final washing buffer

(9 cpm) was also measured by adding 20 µl of the buffer to 3 ml Ultima-Gold scintillation cocktail (PerkinElmer).

2.11 Antibody production and immunohistochemistry

The peptide sequence (PKSASYDMELDNYGKRANQP, GenTel Laboratories, WI, USA) was injected into chickens to raise CmAQP1-specific polyclonal antibodies. The CmAQP1 IgY antibody was then affinity-purified using a SulfoLink™ Immobilization kit for peptides (Thermo Scientific). When the anti-CmAQP1 was omitted, the corresponding secondary anti-chicken IgG caused no non-specific signal.

Due to superious antibody immunoreactivity with the biofilm growing on the cuticle, posterior gills of recently molted seawater acclimated green crabs were sampled. The gills were fixed overnight in 10% neutral buffered formalin (Thermo Scientific) in 2x PBS (Phosphate Buffered Saline, pH 7.4) at 4°C and then stored in 70% reagent alcohol at 4°C. Gills were processed for paraffin embedding, sectioned at 5 µm, and collected onto APS coated slides. Sections were air-dried and dewaxed before staining. Antigen retrieval was performed on sections (0.05% citraconic anhydride, pH 7.3 for 30 min at boiling and 1% SDS/PBS for 5 min at room temperature; see Wilson (2007)) before blocking the sections with 5% normal goat serum in 1% bovine serum albumin TPBS (0.05% tween20/PBS). Sections were then incubated with a combination of chicken anti-AQP and rabbit anti-NKA (Wilson, 2007) primary antibodies diluted at 1:1000 and 1:500, respectively, in 1% BSA/TPBS overnight at 4°C in a humidity chamber. After, sections were rinsed (5, 10, 15 min) and probed with 1:500 dilutions of combined secondary goat anti-chicken Alexa 488 and goat anti-rabbit Alexa 555 antibodies for 1 h at 37°C. Following a final rinse series, and DAPI nuclear staining, coverslips were mounted with 90% glycerol/PBS with 0.05% NaN3. Sections were viewed with a Zeiss Axioscope A1 widefield photomicroscope with an AxioCam MRc colour camera and Zen software. Figures were composed in Adobe Photoshop version 22.5.1.

2.12 Statistics

Statistical analyses were performed using GraphPad Prism Version 9.3.1 (GraphPad Software, San Diego, California USA, www.graphpad.com). The normality of all data was assessed using the Shapiro-Wilk test. Homogeneity of variance was tested using Spearman's test for two-way ANOVAs or Brown-Forsythe test for one-way ANOVAs. Data that were not normally distributed and equally variant were transformed using either Yeo-Johnson, log, or square root transformations to meet the assumptions of parametric statistical tests. Statistical differences in hemolymph and urine osmolality over time upon exposure to 10 ppt. brackish water was determined using a one-way repeated measure ANOVA and a one-way mixed-effect ANOVA, respectively, while differences between hemolymph and urine osmolality at each sampling time point were assessed using a Student's t-test. Changes in hemolymph urea concentrations during hypoosmotic stress were analyzed using an ordinary one-way ANOVA. A Student's t-test was used to compare time 0 urine and hemolymph urea concentrations. A two-way ANOVA was performed to identify statistical differences between the mRNA expression levels of the AQP isoforms of long-term seawater and brackish water acclimated crabs where the independent variables were salinity and tissue type. An ordinary one-way ANOVA test was used to analyze changes in mRNA expression levels of each AQP isoform after 2- and 7-day of exposure to 10 ppt. brackish water. Student's t-tests were used to compare differences between membrane rupture times of oocytes expressing CmAQP1, CmGLP1, CmBIB1, and water-injected oocytes. An ordinary one-way ANOVA was also used to assess differences in the uptake of radioactive urea and data was subsequently tested using the post hoc Dunnet's multiple comparisons test. For all ANOVAs where statistical significance was detected, Tukey's posthoc test was used to make multiple comparisons unless otherwise mentioned. For all data sets, p values < 0.05 were considered significant. Data are presented as means ± standard error (SEM).

3.0 Results

3.1 Changes in hemolymph and urine osmolality after the transfer from sea to brackish water

To examine the effects of short term hypoosmotic stress on hemolymph and urine osmolality, seawater acclimated green shore crabs were transferred from seawater (32 ppt.) to brackish water (10 ppt.) and sampled at 0, 3, 6, 12, 18, 24, 48, and 168 hours (7 days). After 3 hours of exposure to dilute salinity, hemolymph osmolality decreased from an initial (t = 0h) 980.8 ± 3.9 to 900.6 ± 11.2 mOsmol kg^{-1} but remained well above the new ambient environmental osmolality of 298.3 mOsmol kg^{-1} (Fig. 6). Hemolymph osmolality continued to decrease until 48 hours after the transfer (585.2 ± 28.62 mOsmol kg^{-1}) until a slight increase in osmolality was observed thereafter between 48 hours and 7 days (684.6 ± 18.14 mOsmol kg^{-1}, Fig. 6). The osmolality of the urine decreased from 983.5 ± 9.4 to 537.2 ± 36.8 mOsmol kg^{-1} in the first 3 hours after the transfer (Fig. 6) and was hypoosmotic when compared to the hemolymph. Throughout the time course, urine osmolality remained lower than hemolymph osmolality and stabilized after 24 hours with an osmolality of 404.9 ± 38.53 mOsmol kg^{-1}.

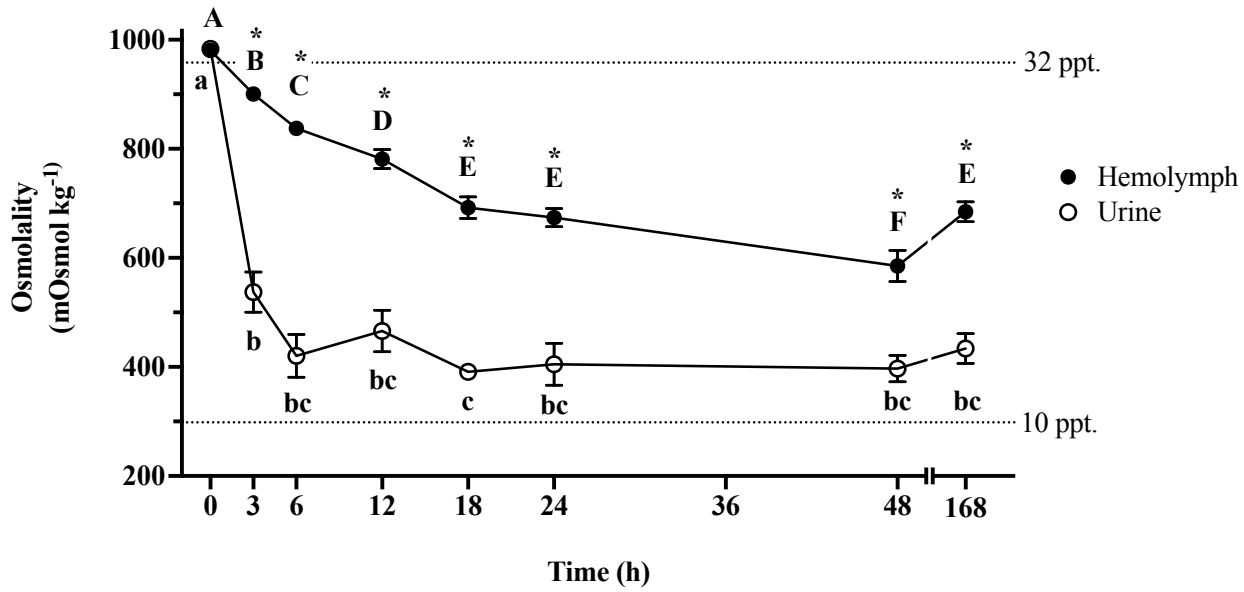

Figure 6: Hemolymph and urine osmolality of seawater acclimated *Carcinus maenas* (top dashed line-32 ppt.) transferred to brackish conditions (bottom dashed line-10 ppt.) over 7 days. Upper-case letters denote differences between time points for hemolymph, lower-case letters denote differences between time points for urine (One-way ANOVA, Tukey's). Asterisks indicate significant differences between urine and hemolymph values at a given time point (Student's T-test). Data presented as means ± S.E.M, $p < 0.05$ (n = 6-8).

3.2 Changes in hemolymph urea concentration after the transfer from sea to brackish water

Seawater acclimated crabs were transferred to dilute seawater conditions (10 ppt.) to determine the effect on hemolymph and urine urea concentrations as a potential osmolyte. Exposure to brackish water conditions (10 ppt.) caused a significant increase in hemolymph urea concentrations from 123.1 ± 17.76 μmol l^{-1} in seawater conditions to 226.5 ± 33.2 μmol l^{-1} after 3 hours of exposure and remained at similar levels over the 7-day tenure of the experiment (Fig. 7). Note, that urea concentrations in the urine measured at time zero were 11.94 ± 4.3 μmol l^{-1} and after the transfer to 10 ppt. were below detectable levels (10 μmol l^{-1}) at all sampling time points thereafter (Fig. 7).

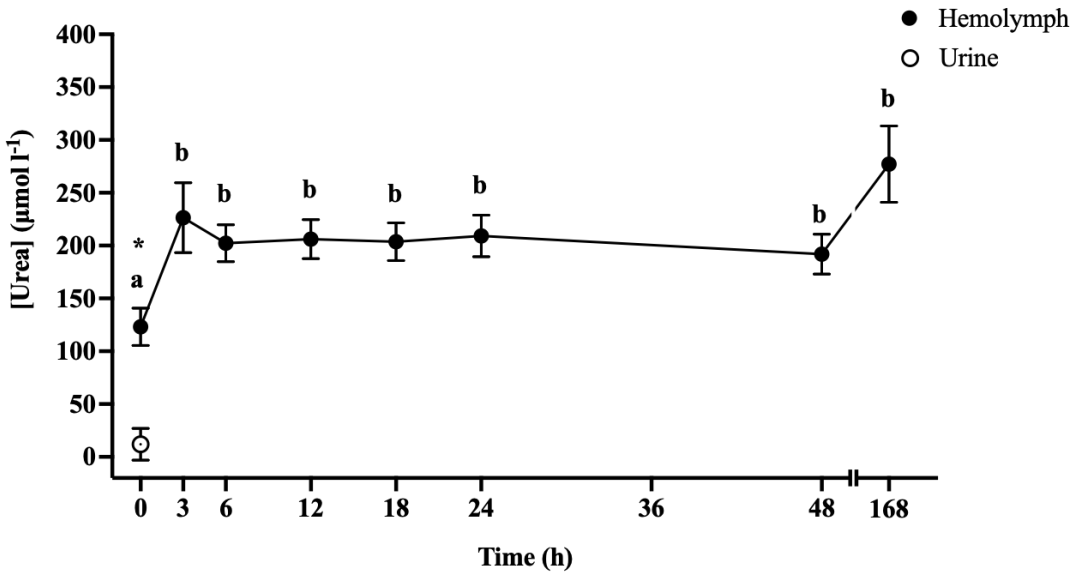

Figure 7: Urea concentrations within the hemolymph and urine of seawater acclimated *Carcinus maenas* (32 ppt.) transferred to brackish water conditions (10 ppt.) over 7 days. Letters denote statistically significant differences between urea concentrations within hemolymph at the given time point. The asterisk indicates a statistically significant difference between urine and hemolymph concentrations at t = 0 h (One-way ANOVA, Tukey's, n = 7-12). Data presented as means ± S.E.M, $p < 0.05$.

3.3 Sequence analyses of Carcinus maenas CmAQP1, CmGLP1 and CmBIB1

To obtain sequence information of these transporters, a publicly available transcriptome of *C. maenas* was mined. Three AQP isoforms were identified in *C. maenas,* and each respective mRNA sequence was cloned using gene-specific primers targeting the open reading frame. This resulted in putative AQP coding open reading frames consisting of 780 base pairs (CmAQP1), 930 base pairs (CmGLP1), and 1014 base pairs (CmBIB1) encoding proteins of 259 aa (CmAQP1), 309 aa (CmGLP1), and 337 aa (CmBIB1). Amino acid analyses showed that each AQP isoform exhibits the conserved AQP family signatures including, six transmembrane helices which are connected by five loops (A – E) and two conserved asparagine–proline–alanine (NPA) motifs. The deduced amino acid sequences of *Carcinus maenas* include the classical aquaporin (CmAQP1, Genbank: ON416879), aquaglyceroporin (CmGLP1, Genbank: ON416880), and big brain protein (BIB) (CmBIB1, Genbank: ON416881) are now published on GenBank. The two highly conserved hydrophobic stretch regions containing the two NPA motifs that are involved in forming each monomer's pore were identified in all three isoforms. The CmBIB1 isoform had one NPA motif conserved at the second location (265-267 aa), while the first NPA location site (219-221 aa) has two amino acid substitutions of S219 and P221. Additionally, phosphorylation sites were predicted for CmAQP1 (S202), CmGLP1 (T48, S161, Y217, S290) and CmBIB1 (T26, S44, S65, T93, S162, S223, T303, T323, S324, S335). No signal peptides were identified for any of the three identified AQP sequences.

A Maximum Likelihood analysis revealed that the three identified *C. maenas* aquaporins clustered in separate subfamilies of AQPs (Fig. 8). One *C. maenas* isoform clustered with other malacostracans (shrimp and lobster) classical aquaporins (AQPs), the largest subfamily of AQPs. The second isoform clustered with other known crustacean aquaglyceroporins (GLPs) and is most similar to that of the *Daphnia magna* GLP. The third isoform is clustered with a subfamily of neurogenic big brain channel proteins (BIBs) that is only known in arthropod lineages (Fig.8).

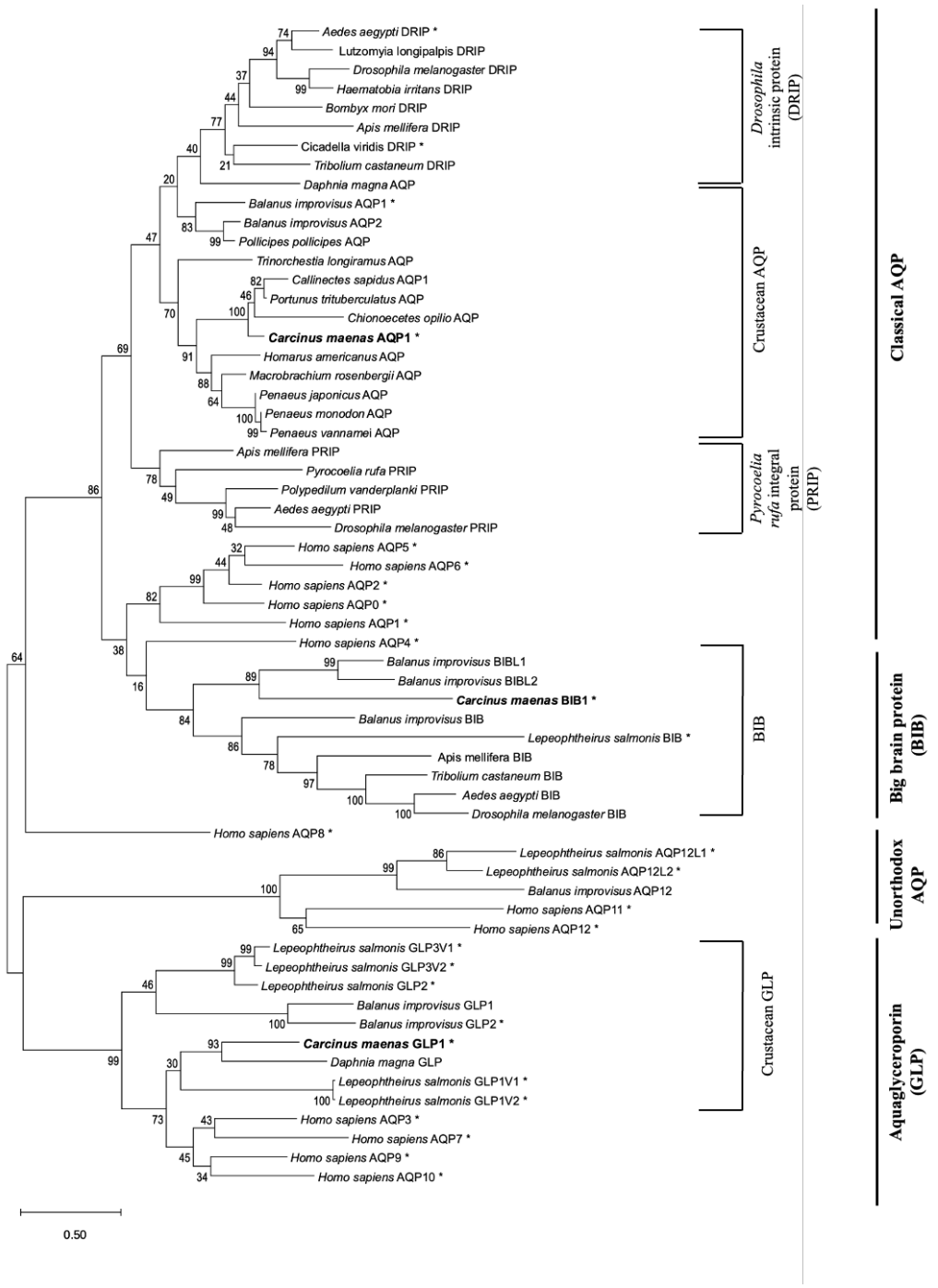

Figure 8: Sequence homology analysis of aquaporin (AQPs) proteins. Inferred by using the Maximum Likelihood method and JTT matrix-based model (Jones et al., 1992). Bolded text indicates proteins investigated in this study (*Carcinus meanas* aquaporins: CmAQP1, CmGLP1 and CmBIB1). The asterisks indicate that the proteins have been functionally characterized (for references refer to Table 3). The tree with the highest log likelihood (-35059.02) is shown. The tree is drawn to scale, with branch lengths measured in the number of substitutions per site.

3.4 Tissue-specific expression at long term acclimated seawater and brackish water conditions

To analyze tissue-specific expression, absolute expression values of *C. maenas* AQPs were evaluated by qPCR in gills, antennal glands, claw muscle, hindgut epithelial cells, and ganglia of crabs either long-term acclimated to a salinity of 32 ppt. or 10 ppt. (Fig. 9).

The classical AQP, CmAQP1, was found to be expressed in all tissues tested with the highest expression in the hindgut and ganglia, followed by the claw muscle, ganglia, antennal glands, anterior gill 5, and posterior gill 8 (Fig. 9A). In seawater conditions, mRNA expression levels of CmAQP1 were very low in posterior gill 8, specifically, ca. 2822 times lower than the transcript's expression levels detected in the hindgut. In brackish water conditions, the same general expression pattern was observed with the highest expression in the hindgut and ganglia with the lowest in the posterior gill 8. When crabs were long-term acclimated to a salinity of 10 ppt., transcript levels of CmAQP1 were downregulated in all tissues examined compared to levels observed in seawater acclimated individuals. Of note, in the osmoregulatory active antennal glands and posterior gills, transcript expression levels of CmAQP1 were massively downregulated by 95% and 97%, respectively, in brackish water acclimated animals when compared to seawater conditions. Localization studies employing CmAQP1-specific antibodies revealed that this classical AQP has an apical/subapical localization in the posterior gills of seawater acclimated crabs. In parallel, the anti- Na^+/K^+-ATPase (α-subunit) antibodies confirmed the basolateral localization of this enzyme (Fig. 10).

Transcripts of the aquaglyceroporin, CmGLP1, were also found in all investigated tissues (Figs. 9B). When crabs were long-term acclimated to a salinity of 32 ppt., the ganglia had the highest mRNA expression, followed by the antennal glands, claw muscle, hindgut, and gills. The lowest expression of CmGLP1 was seen in posterior gill 8 which was expressed at 39 times lower levels than the ganglia. Similar to CmAQP1, CmGLP1 transcripts were downregulated in all tissues examined in crabs that were long-term acclimated to brackish water compared to their seawater acclimated counterparts.

Transcripts encoding the big brain protein isoform (CmBIB1) were also detected in all tissues investigated (Fig. 9C). When crabs were long-term acclimated to a salinity of 32 ppt., the ganglia showed the highest expression followed by the antennal glands, hindgut, and the claw muscle while the anterior and posterior gills were of intermediate expression and statistically

similar to all tissues. It is noteworthy that transcript levels for branchial expressed CmBIB1 are ca. 45-times higher when compared to expression levels of CmAQP1 and CmGLP1 in seawater acclimated individuals. Additionally, long-term acclimation of crabs to a salinity of 10 ppt., caused downregulation of CmBIB1 mRNA levels in all investigated tissues when compared to the expression levels of seawater acclimated individuals.

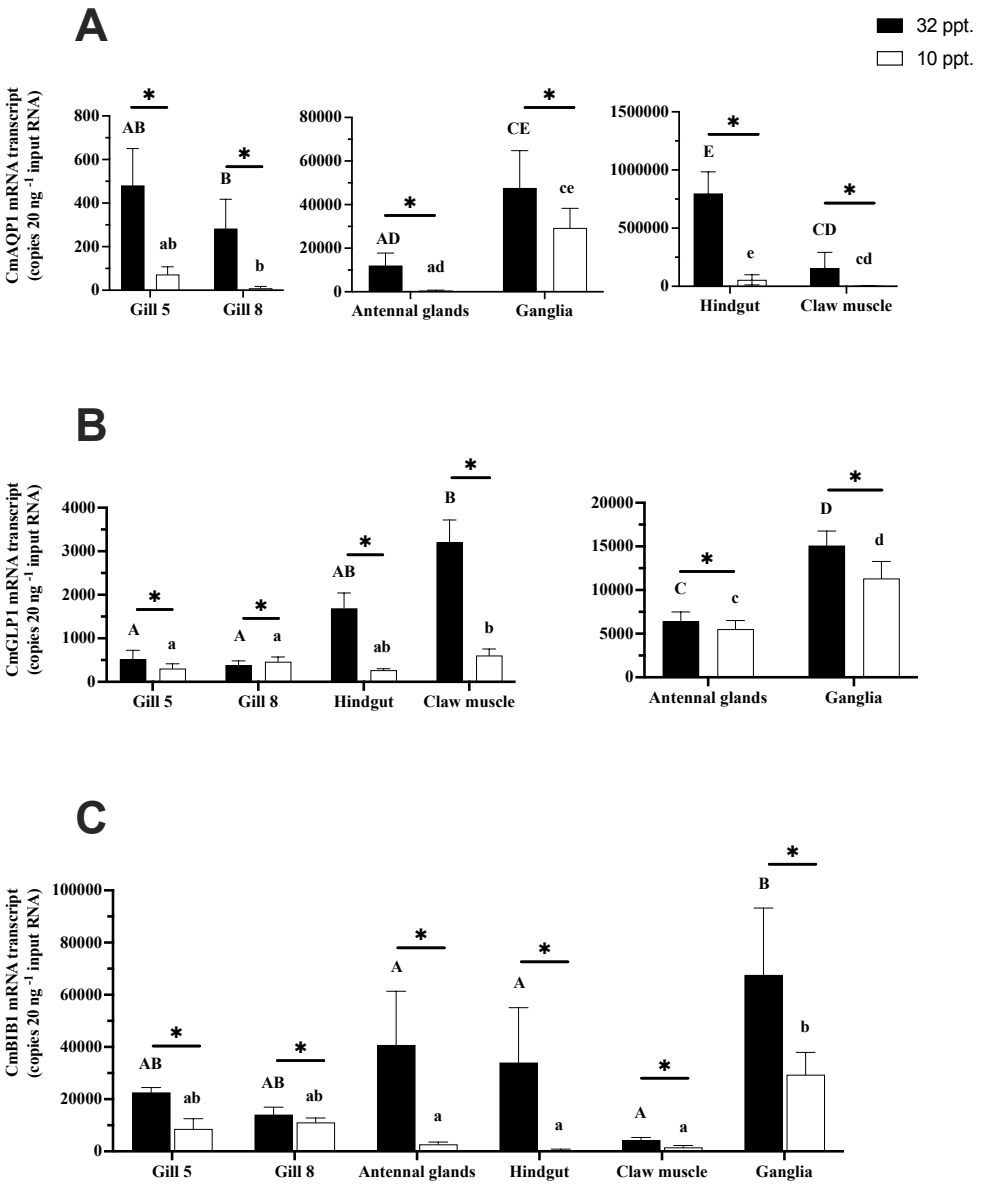

Figure 9: Absolute mRNA expression levels of *Carcinus maenas* aquaporins: CmAQP1 (A), CmGLP1 (B), and CmBIB1 (C) from individuals acclimated long-term to a salinity of 32 ppt. or 10 ppt. The asterisks indicate significant differences between mRNA expression in 32 ppt. and 10 ppt. Capital letters denote significant differences between 32 ppt. acclimated tissues, while lower case letters denote significant differences between 10 ppt. acclimated tissues (Two-way ANOVA, Tukey, $P \leq 0.05$, n = 5-7). Data are presented as means ± SEM.

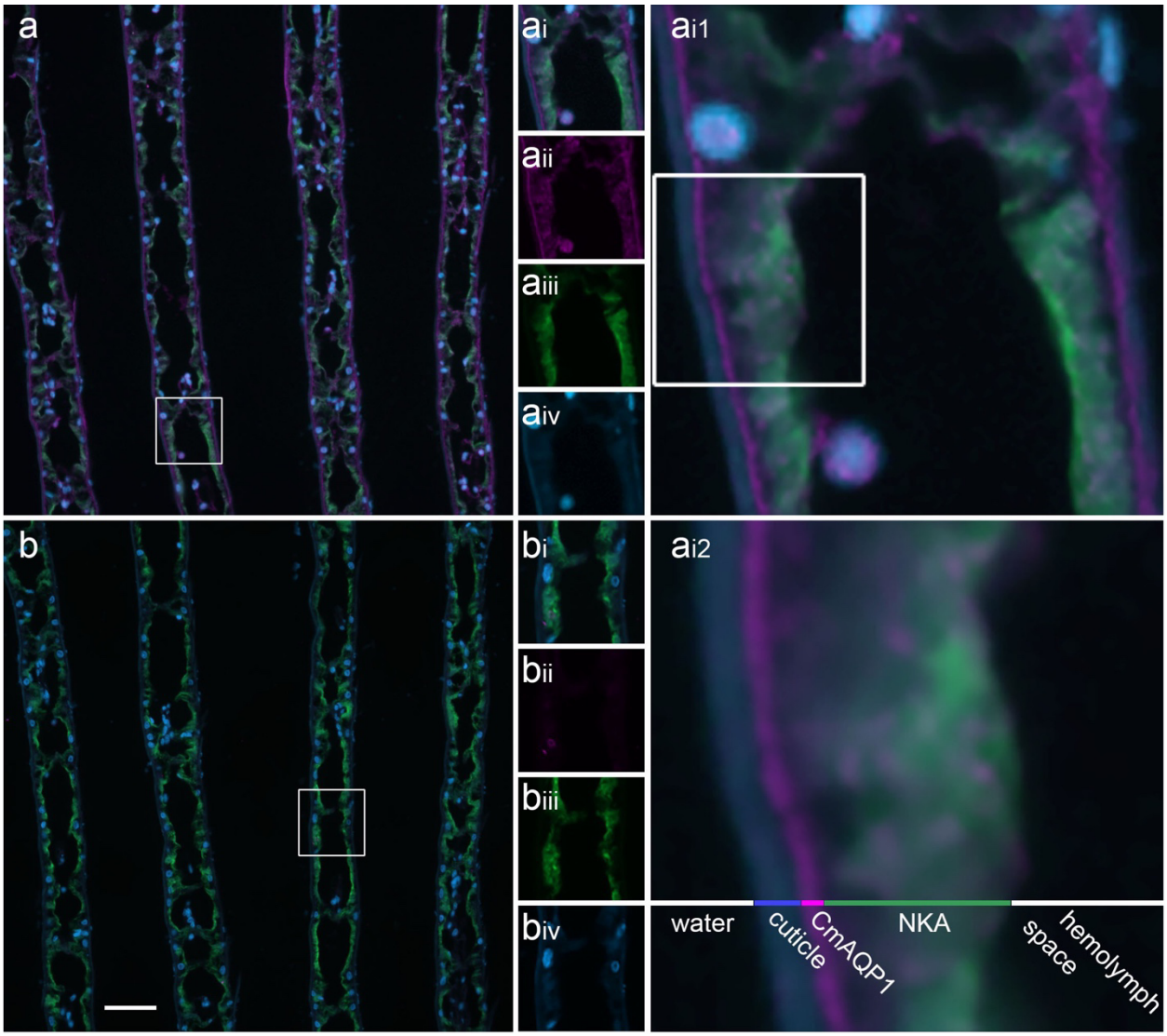

Figure 10: (a) Immunohistochemical localization of CmAQP1 (magenta) with NKA (green) in the posterior gills of a recently molted *Carcinus maenas*. (a/ai) merged image displaying CmAQP1, NKA and DAPI. Insets (ai, bi) are presented on the side at an additional 2x magnification with colour channels separated (aii) CmAQP1, (aiii) NKA, (aiv) DAPI. (b,bi-iv). The equivalent to image (a,ai-aiv), but with the omission of the primary antibody targeting CmAQP1. Panel ai was further enlarged an additional 4x (ai1) and 16x (ai2) to show the detailed localization of CmAQP1. Scale bar (a,b) 50 µm (ai-iv,bi-iv) 25 µm, (ai1) 6.25µm, (ai2) 1.56µm.

3.5 Effects of acute low salinity exposure on CmAQP1, CmGLP1, and CmBIB1 mRNA expression in osmotic active gills and antennal glands

To investigate if CmAQP1, CmGLP1, and CmBIB1 are involved in osmoregulation, changes in their mRNA expression levels were determined in the osmoregulatory active gills and

the antennal glands at 2- and 7-days post-transfer from 32 ppt. salinity to 10 ppt. mRNA expression levels of CmAQP1 were unaffected in anterior and posterior gills after 2 and 7 days of exposure to a dilute environment (Fig. 11A). In contrast, expression levels of CmAQP1 decreased in the antennal glands after transferring the animals to 10 ppt. (Fig. 11B). Transcript expression levels of CmGLP1 decreased in the anterior gill following 2 and 7 days of exposure to the dilute conditions whereas expression within the posterior gills and antennal glands were unaffected (Fig. 11B). The CmBIB1 transcript levels were downregulated in both the anterior gill 5 and posterior gill 8 in low salinity but remained unchanged in the antennal glands (Fig. 11C).

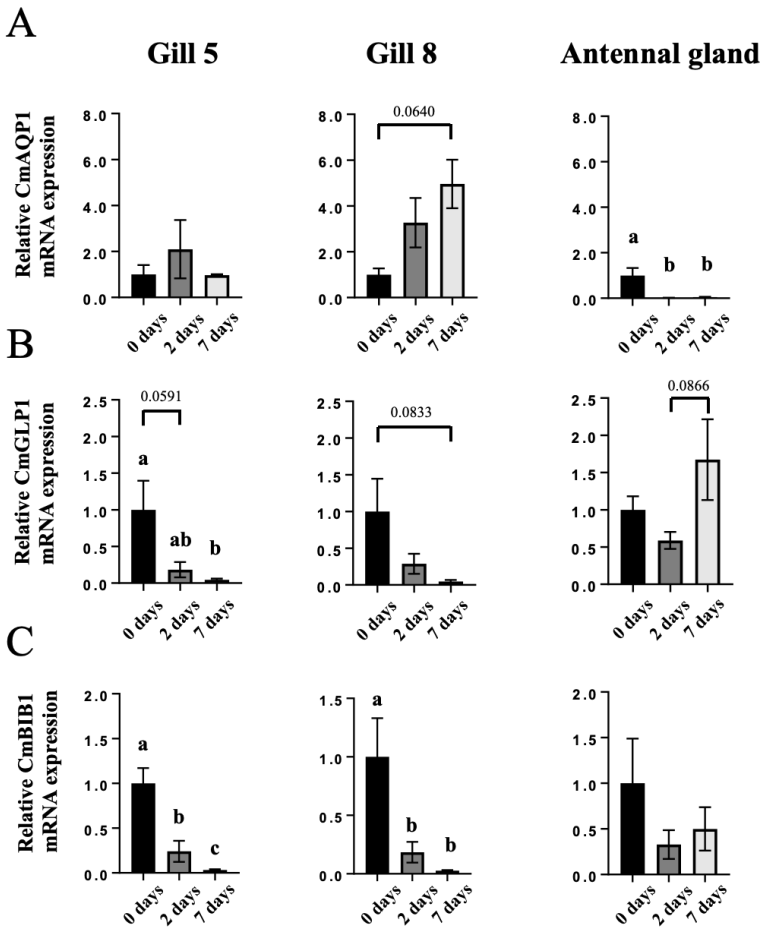

Figure 11: Relative mRNA expression levels of *Carcinus maenas* aquaporins: CmAQP1 (A), CmGLP1 (B), and CmBIB1 (C) in anterior gill 5, posterior gill 8 and the antennal gland from seawater (32 ppt.) acclimated individuals (0 days) exposed to brackish conditions (10 ppt.) for 2 or 7 days. The letters indicate significant differences between sampling time points. (Ordinary one-way ANOVA, Tukey, $P \leq 0.05$, n = 5-7). Data are presented as means ± SEM.

3.6 Functional analysis of the water permeability of CmAQP1, CmGLP1, and CmBIB1

To corroborate the Maximum Likelihood and theoretical structural analyses, the functional permeation properties of the three identified AQP isoforms were examined by heterologous expression in *Xenopus laevis* oocytes followed by measurements of the oocyte osmotic water permeability in media that is hypoosmotic relative to their expected intracellular osmolality.

Video analysis revealed that oocytes injected with CmAQP1 ruptured after 9 ± 2.4 seconds (n = 9), while CmGLP1 expressing oocytes ruptured after 62 ± 17.7 seconds (n = 5). In contrast, oocytes injected with CmBIB1 did not indicate water transport over the oocyte cell membrane, with no rupture occurring after 1 hour in hypoosmotic stress, which was equal to measurements of the water-injected control oocytes (n = 5, Fig. 12). In addition, CmAQP1 was sensitive to $NiCl_2$ (1 mmol l^{-1}), which prolonged the time to rupture to 210 ± 51.5 seconds. The application of 1 mmol l^{-1} $NiCl_2$ had no effects on the time to rupture in CmGLP1 expressing oocytes or the respective water-injected control oocytes (n = 5). Data not shown.

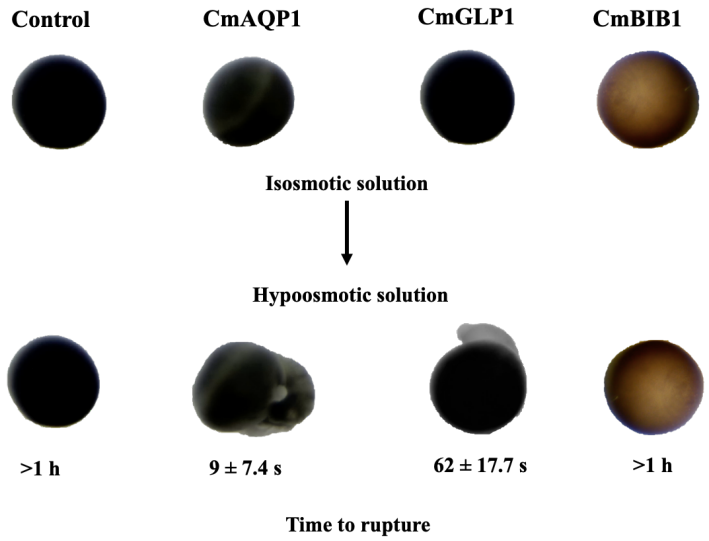

Figure 12: Representative functional demonstration of water transport capabilities of *Carcinus maenas* aquaporins: CmAQP1, CmGLP1, and CmBIB1 expressed in *Xenopus laevis* oocytes. Top panel from left to right: water-injected control oocyte (n = 5) and oocyte expressing CmAQP1 (n = 9), CmGLP1(n = 5) or CmBIB1 (n = 5). Bottom panel: respective oocytes after transfer to the hypoosmotic solution.

3.7 Functional analysis of the urea permeability of CmAQP1, CmGLP1, and CmBIB1

The absence of urea in the collected final urine and the presence of CmAQP1, CmGLP1, and CmBIB1 in the antennal gland suggested the potential participation of these AQP isoforms in the retention of urea in this tissue. To investigate this further, urea transport capabilities of all three isoforms were examined by heterologous expression in *Xenopus laevis* oocytes followed by measurement of uptake of radioactive urea. As shown in figure 13, only the CmGLP1-expressing oocytes had consistently higher urea uptake rates than those of controls (water-injected), while CmAQP1 and CmBIB1 were indifferent from controls (n = 6-9). Urea and water transport by CmGLP1-expressing oocytes was not sensitive to 1 mmol l^{-1} $NiCl_2$ (Fig. 15).

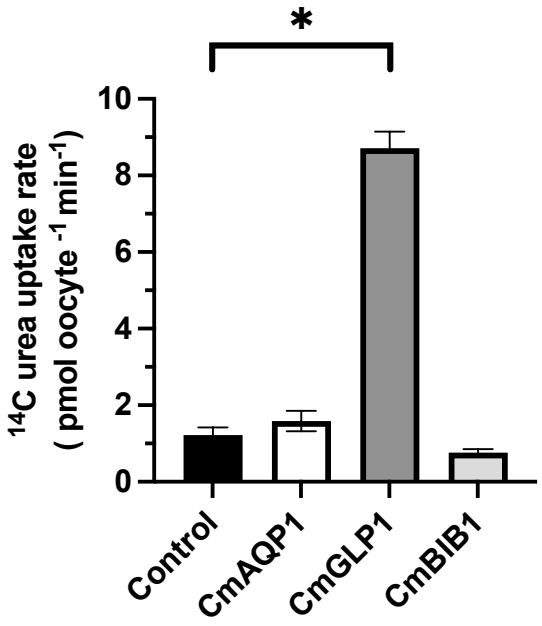

Figure 13: Uptake of ^{14}C urea in *Xenopus laevis* oocytes expressing *Carcinus maenas* aquaporins: CmAQP1, CmGLP1, and CmBIB1 after a 30-minute incubation period. Asterisks denote significant differences between control and CmGLP1 expressing oocytes (One-way ANOVA, Dunnet's $P < 0.0001$, n = 6).

4.0 Discussion

4.1 Changes in hemolymph and urine osmolality and urea content after the transfer from sea to brackish water

When seawater acclimated green shore crabs move to brackish water, the osmotic gradient between the hemolymph and environment promotes both an influx of water and efflux of ions across the crab's epithelium (Henry et al., 2012). Although studies have clearly identified the posterior gills of *C. maenas* as the main site of active ion absorption in dilute environments, their means of eliminating excess water from their body fluids are poorly defined. As shown in figure 6, *C. maenas* excretes excess water through the production of hypoosmotic urine upon hypoosmotic stress, as documented in other decapods inhabiting hypoosmotic environments. These decapod species include the euryhaline crayfish *Pacifastacus leniusculus,* the larval mangrove crabs *Scylla tranquebarica*, and the striped shore crab, *Pachygrapsus crassipes* (Prosser and Green, 1955; Misbah et al., 2017; Wheatly and Henry, 1987).

Urea can be used by animals as a non-ionic osmolyte to adjust the osmolality of urine and thereby change the amount of water being excreted, as occurs during diuretic and antidiuretic regulatory processes in the mammalian kidneys (Fenton, 2009; Higgins, 2016). Luminal urea within the mammalian nephron becomes progressively concentrated, peaking within the distal regions of the collecting duct. The concentrated urea creates an osmotic gradient that directs luminal water through aquaporins expressed within the collecting duct's apical and basolateral epithelium resulting in the conservation of body water (Sands et al., 2010). When the blood is near osmotic homeostasis, the concentrated urea is passed into the bladder for excretion. When a mammal's blood is too concentrated, circulating concentrations of antidiuretic hormone (ADH) rise, causing urea transporters to be inserted into the terminal inner medullary collecting duct causing luminal urea to be recycled from the collecting duct into the thin ascending limb of Henle rather than being freely passed into the bladder for excretion. Recycled urea increases the magnitude of urea concentrated within the collecting duct lumen, thereby increasing the amount of water reabsorbed into the bloodstream (Sands et al., 2010). Aquatic crustaceans are ammonotelic and, unlike mammals whose plasma urea concentrations range between 2.5 – 7.8 mmol l^{-1} hemolymph urea concentrations of *C. maenas* have been reported to be very low,

ranging from 0–80 μmol l^{-1} in seawater-acclimated crabs to 600–1000 μmol l^{-1} in crabs long-term acclimated to 10 ppt. salinity (Weihrauch et al., 2009). The increase in systemic urea concentrations upon acclimation to dilute salinities may be related to the increased metabolic demand and nitrogenous waste production associated with osmoregulation. The biological significance of urea in crustaceans is poorly understood, although a recent study has suggested it may be produced to mitigate high ammonia loads following feeding; however, the study did not address the fact that the urea may be the result of arginolysis rather than a detoxification mechanism (Quijada-Rodriguez et al., 2022). In the current study, we showed that hemolymph urea concentrations increased by 56% upon acute hypoosmotic stress; however, the overall hemolymph concentration of ca. 277 μmol l^{-1} seems too low to be considered a crucial systemic osmolyte in *C. maenas*. Although systemic levels were low, it was observed that urea was absent in the final urine of brackish water acclimated animals and only lowly concentrated (11.94 ± 4.32 μmol l^{-1}) in the urine of seawater animals (Fig. 7). This suggests that the antennal glands possess a previously undescribed mechanism to reabsorb and retain urea rather than excrete it into the environment, potentially as a means to manipulate the osmolality of the final urine. While speculative and currently lacking mechanistic evidence, this mechanism may entail the concentration of urea within the filtrate may draw excess water from the hemolymph into the antennal gland lumen while the insertion of urea transporters, possibly including the urea-permeable CmGLP1 as discussed below, at the distal region of the antennal gland or even the bladder allows urea to be recycled to create a dilute and urea-poor final urine.

4.2 Potential osmoregulatory role of CmAQP1

Sequence homology revealed that CmAQP1 is likely a classical water-transporting AQP, clustering with the classical AQPs of other brachyurans. The closest homology of a functionally characterized classical AQP is that of the bay barnacle (*B. improvises)* AQP1. Both the classical AQP of the bay barnacle and CmAQP1 demonstrated an ability to transport water (Lind et al., 2017; Fig. 12). Additionally, water transport by CmAQP1 was also found to be Ni2+ sensitive when heterologously expressed within *Xenopus* oocytes.

The CmAQP1 was ubiquitously expressed in all tissues examined but showed the highest transcript levels in hindgut epithelial cells. The osmoregulatory role of the gastrointestinal tract

of crustaceans has rarely been studied; however, it can be presumed that its organs contribute to the animal's osmotic state given their transport of solutes and water that must occur to absorb dietary nutrients (McGaw and Curtis, 2013; McNamara et al., 2005; Whittamore, 2012). In fish species such as the Atlantic salmon (*Salmon salar*), European eel (*Anguilla Anguilla*), Japanese eel (*Anguilla japonica*), and the seabass (*Dicentrarchus labrax*), differential expression of AQPs along the gastrointestinal tract regulates the amount of water that follows the absorbed nutrients and plays a determining role in the gastrointestinal net water flux (Whittamore, 2012). More specifically, AQP1 mRNA and protein expression has been shown to increase towards the distal portions of the intestine of these teleost species. The localization of AQP1 to the apical brush border of the intestine in seawater acclimated species would imply a potential role for AQP1 in regulating water absorption in the distal regions of the intestine (Whittamore, 2012). The high mRNA abundance in the hindgut suggests that CmAQP1 plays a dominant role in regulating water transport within the hindgut of the green shore crab as well. Moreover, due to its ubiquitous expression pattern, we hypothesize that CmAQP1 also plays a role in cellular and systemic osmoregulatory processes, indicated by the downregulation of this channel in all of the investigated tissues.

In dilute seawater, *C. maenas* becomes an osmoregulator (Fig. 6; Henry, 2005; Nagel, 1934) by actively absorbing Na^+ and Cl^- across its gills. Concentrating ions within the hemolymph creates an inwardly directed osmotic gradient and thereby draws water across their moderately leaky epithelia into the hemolymph (Freire et al., 2008; Weihrauch et al., 1999a). Under these conditions, water and ion fluxes must be carefully controlled, presumably through changes in the expression of water channels within the tissues. In line with this hypothesis, our findings show that CmAQP1 mRNA expression levels are reduced in all investigated tissues upon long-term acclimation to brackish water conditions compared to those of seawater acclimated animals (10 ppt., Fig. 9). In the antennal glands, the observed down-regulation of CmAQP1 implicates a reduction in water permeability of the antennal glands and could thereby play a crucial role in the production of dilute urine (Fig. 6). In contrast to the internal tissues, the gills of *C. maenas* are in direct contact with the environment and therefore act as a direct route of water permeation between the animal and the environment upon osmotic stress. When *C. maenas* is osmoconforming in seawater, CmAQP1 is localized to the apical membrane of the posterior gills and may be involved in cell volume regulation of branchial epithelial cells. Intracellular

osmolality should mirror that of the animal's extracellular fluid regardless of its environment (Gilles and Péqueux, 1981). In seawater, the environment, intracellular, and extracellular fluids are approximately equal in osmolality; however, non-osmoregulatory transport processes still occur and can create small osmotic differences between the fluids (Gilles and Péqueux, 1981). The higher overall ubiquitous mRNA expression of CmAQP1 in seawater acclimated crabs represents a means to quickly equilibrate small osmotic gradients developed by non-osmoregulatory processes within the crab as part of general cell volume regulation. The apical localization of CmAQP1 within the gills would allow the channel to equilibrate differences developed along the apical branchial epithelium, whereas other isoforms whose localization has yet to be confirmed are likely present along the basolateral epithelium. In dilute environments, crabs would need to limit the rate that water equilibrates across the tissues, especially organs in contact with the environment or that produce a hypoosmotic fluid such as the gills and antennal glands, respectively. As such, it is logical that the general mRNA expression levels are reduced across the tissues as crabs are acclimated to long-term dilute environments (Fig. 6) resulting in a widespread reduction in water permeability that is crucial for maintaining the osmotic gradient between the bodily fluids and ambient environment. Similar findings have been made in the barnacle *B. improvisus* whose AQP1 expression levels change in response to hypoosmotic stress. Here, the *B. improvisus* classical water-transporting aquaporin, AQP1, exhibited a drastic decrease in expression within the mantle (Lind et al., 2017). It was hypothesized that this mechanism may be used to reduce the influx of water across the mantle into the hyperosmotic hemolymph when inhabiting low salinity environments.

While some populations are chronically exposed to low salinities and permanently inhabit dilute environments such as the Baltic Sea, *C. maenas* also experience acute short-term salinity challenges while inhabiting tide pools and tidal shifts along the coasts (Truchot, 1988). In addition to our long-term exposure experiments, we also investigated the effects of short-term exposure (2 and 7 days) to low salinities on the mRNA expression levels of CmAQP1 in the osmoregulatory active tissues - the gills and antennal glands. In contrast to the effects observed after long-term exposure to low salinities, acute exposure did not affect the transcript expression levels of CmAQP1 in the anterior or posterior gills. It must be noted that the overall mRNA expression levels of CmAQP1 are very low in both gill types, making it difficult and rather speculative to discuss the potential biological significance of these results. Regardless, our

results contrast with those of a previous study that found that larval blue crabs, *C. sapidus*, increase the transcription of a classical aquaporin, AQP1, during short-term (96 hours) exposure to low salinity (15 ppt., Chung et al., 2012). Further investigations, including potential changes in expression at the protein level, are needed to clarify the short-term effects of dilute environments on classical AQP proteins in osmoregulating crustaceans.

4.3 Potential osmoregulatory role of CmGLP1

Sequence homology revealed that CmGLP1 is likely an aquaglyceroporin, potentially transporting water and other small solutes including urea. In the present study, CmGLP1 was found to function as a water and urea channel, similar to other crustacean GLPs (Lind et al., 2017; Stavang et al., 2015). The highest expression in seawater acclimated animals was found within the ganglia and antennal glands. The high mRNA expression levels within the antennal glands and the absence of urea in the final urine of brackish water acclimated animals may indicate that CmGLP1 is involved in a previously undescribed diuretic urea reabsorption process within the antennal glands. Although purely hypothetical, urea may be concentrated within the early portions of the antennal gland allowing excess water to be drawn into the lumen. Later portions of the antennal gland may then reabsorb urea, through CmGLP1 and/or other urea transporters, resulting in the expulsion of hypoosmotic urea-poor final urine. This process may also extend to the bladder, if present, which has been shown to have ion-transporting capabilities in the *Dungeness* crab (Holliday, 1980). In long-term brackish water acclimated crabs circulating urea concentration can reach ca. 1 mmol l^{-1} (Weihrauch et al., 2009), while urea concentrations in particular regions of the antennal glands may be even higher, as observed e.g. in the inner medulla of the mammalian kidneys, where urea concentrations of up to 100-200 mmol l^{-1} are observed (Pennell et al., 1975). Clearly, more investigations with regards to the role of urea transporters and urea itself in the production of dilute urine by the antennal gland are needed in the future.

Aside from the antennal glands, CmGLP1 was also downregulated in the gills, claw muscle, hindgut and ganglia under long-term acclimation to brackish conditions in comparison to seawater acclimated crabs. Due to CmGLP1's ability to transport both water and urea, identifying its potential physiological roles in a variety of tissues is more complex. In contrast to

CmAQP1, the mRNA abundance of CmGLP1 was downregulated as early as 7-days of exposure to brackish conditions in branchial tissues. It has been previously identified that when gills of brackish water (10 ppt.) acclimated *C. maenas* are perfused with 600 µmol l^{-1} of urea, the 600 µmol l^{-1} of urea remained within the final perfusate (Weihrauch, personal communication). This would indicate that the gills are tight for urea, as would be desirable if the molecule is involved in maintaining an osmoregulating state in dilute media. The low urea-permeability of the gill would strengthen the hypothetical basolateral localization of CmGLP1 in the tissue which may benefit the animal by promoting the retention of urea as an osmolyte that could be recycled as occurs within the distal region of the mammalian nephron. In comparison to CmAQP1, the overall mRNA abundance of CmGLP1 was much lower in non-branchial tissues and may serve to reduce the tissues' water permeability and retain intracellular urea as an osmolyte.

4.4 Potential osmoregulatory role of CmBIB1

Sequence analysis indicated that CmBIB1 belongs to the arthropod-specific aquaporin subfamily called big brain (BIB) proteins. The identified CmBIB1 was most similar to that of the *B. improvisus* BIB- like 2 (BIBL-2) isoform and *L. salmonis* BIB. Similar to the findings from the current study on CmBIB1, heterologous expression of the *L. salmonis* BIB in *Xenopus* oocytes demonstrated that the channel does not transport water or urea (Stavang et al., 2015). While a BIB in *Drosophila* has also been reported not to promote water transport, mutagenesis experiments have determined that this *Drosophila* BIB is important for the neural development in the embryonic brain, and potentially plays a role in the development/functioning of the nervous system (Rao et al., 1990). In fact, *Drosophila* BIB has been shown to have an ion-conductance (Na^+ and K^+) and certain cell-adhesion properties (Tatsumi et al., 2009; Yanochko and Yool, 2002). These described properties in the fruit fly in combination with the downregulation observed in all investigated tissues in crabs acclimated to a low salinity environment suggest a potential role of CmBIB1 in osmoregulation through the modification of the cellular or epithelial ion conductivity. Due to CmBIB1's high tissue mRNA abundance and its downregulation in response to dilute conditions, future studies should investigate the potential role of big-brain proteins in osmoregulation.

5.0 Conclusions

This study is the first to reveal the substrate permeability properties of AQPs in a decapod crustacean and broadens the understanding of the osmoregulatory role of AQPs in aquatic invertebrates. Here, we presented three different subfamilies of AQPs - the classical AQPs, the aquaglyceroporins, and the arthropod-specific big brain proteins. CmAQP1 and CmGLP1 were found to transport water and are both expressed at the mRNA level in osmoregulatory and non-osmoregulatory cells. The mRNA expression of these channels both responded to osmotic stress, suggesting that these AQPs are involved in osmohomeostasis of the body fluids and anisosmotic cell volume regulation. The physiological role of CmBIB1 is more obscure as its substrates have not been identified yet. Due to its ubiquitous expression pattern and its sensitivity to changes in the environmental and extracellular osmolality, it is possible that CmBIB1 acts as a cation channel (Tatsumi et al., 2009; Yanochko and Yool, 2002) that is directly related to cell volume regulation.

Although three different types of AQP isoforms were identified in the current study, this investigation represents the beginning of our understanding of AQPs regarding their presence, role, and physiological function in decapod crabs and crustaceans in general. Furthermore, our results suggest that urea is reabsorbed by the antennal gland and potentially recycled as part of the mechanism that produces dilute urine. This hypothetical mechanism would involve the concentration of urea within the proximal regions of the antennal glands to draw water into the lumen and the reabsorption of urea, but not water, in the distal regions of the glands similar to mechanisms present in the mammalian kidney. Physiological experiments and functional expression analysis of any identified AQP must be conducted to place these proteins into a biological context.

6.0 References

Agre, P., 2004. Aquaporin water channels (nobel lecture). Angew. Chemie - Int. Ed. 43, 4278–4290.

Agre, P., Kozono, D., 2003. Aquaporin water channels: Molecular mechanisms for human diseases. FEBS Lett. 555, 72–78.

Agre, P., Preston, G.M., Smith, B.L., Jung, J.S., Raina, S., Moon, C., Guggino, W.B., Nielsen, S., 1993. Aquaporin CHIP: the archetypal molecular water channel. Am. J. Physiol. Physiol. 265, 463-476.

Akhter, H., Misyura, L., Bui, P., Donini, A., 2017. Salinity responsive aquaporins in the anal papillae of the larval mosquito, *Aedes aegypti*. Comp. Biochem. Physiol. -Part A Mol. Integr. Physiol. 203, 144–151.

Allen, G.J.P., Wang, M.-C., Tseng, Y.-C., Weihrauch, D., 2021. Effects of emersion on acid–base regulation, osmoregulation, and nitrogen physiology in the semi-terrestrial mangrove crab, *Helice formosensis*. J. Comp. Physiol. B Biochem. Syst. Environ. Physiol. 191, 455–468.

Benga, G., 2012. The first discovered water channel protein, later called aquaporin 1: molecular characteristics, functions and medical implications. Mol. Aspects Med. 33, 518–534.

Benga, G., 1988. Water transport red blood cell membranes. Prog. Biophys. Mol. Biol. 51, 193–245.

Benga, G., Popescu, O., Borza, V., Pop, V., Muresan, A., Mocsy, I., Brain, A., Wrigglesworth, J.M., 1986. Water permeability in human erythrocytes: identification of membrane proteins involved in water transport. Eur. J. Cell Biol. 41, 252–262.

Campbell, E.M., Ball, A., Hoppler, S., Bowman, A.S., 2008. Invertebrate aquaporins: A review. J. Comp. Physiol. B Biochem. Syst. Environ. Physiol. 178, 935–955.

Cerdà, J., Finn, R.N., 2010. Piscine aquaporins: an overview of recent advances. J. Exp. Zool. Part A 313, 623–650.

Chamberlin, M.E., Strange, K., 1989. Anisosmotic cell volume regulation: a comparative view. Am. J. Physiol. - Cell Physiol. 257, C159–C173.

Chou, C.L., Tonghui, M., Yang, B., Knepper, M.A., Verkman, A.S., 1998. Fourfold reduction of water permeability in inner medullary collecting duct of aquaporin-4 knockout mice. Am. J. Physiol. Physiol. 274, C549–C554.

Chung, J.S., Maurer, L., Bratcher, M., Pitula, J.S., Ogburn, M.B., 2012. Cloning of aquaporin-1 of the blue crab, *Callinectes sapidus*: its expression during the larval development in hyposalinity. Aquat. Biosyst. 8, 1–10.

Compere, P., Wanson, S., Pequeux, A., Gilles, R., Goffinet, G., 1989. Ultrastructural changes in the gill epithelium of the green crab *Carcinus maenas* in relation to the external salinity. Tissue cell 22, 299–318.

Compton, T.J., Leathwick, J.R., Inglis, G.J., 2010. Thermogeography predicts the potential global range of the invasive European green crab (*Carcinus maenas*). Divers. Distrib. 16, 243–255.

Copeland, D.E., Fitzjarrell, A.T., 1968. The salt absorbing cells in the gills of the blue crab (*Callinectes sapidus* rathbun) with notes on modified mitochondria. Zeitschrift für Zellforsch. und Mikroskopische Anat. 92, 1–22.

Delaunay, H., 1931. L'excretion azotee des invertebres. Philos. Soc. Rev. Camb. 6, 265–301.

Denker, B.M., Smith, B.L., Kuhajda, F.P., Agre, P., 1988. Identification, purification, and partial characterization of a novel M(r) 28,000 integral membrane protein from erythrocytes and renal tubules. J. Biol. Chem. 263, 15634–15642.

Doherty, D., Jan, L.Y., Jan, Y.N., 1997. The *Drosophila* neurogenic gene big brain, which encodes a membrane-associated protein, acts cell autonomously and can act synergistically with Notch and Delta. Development 124, 3881–3893.

Drake, L.L., Rodriguez, S.D., Hansen, I.A., 2015. Functional characterization of aquaporins and aquaglyceroporins of the yellow fever mosquito, *Aedes aegypti.* Sci. Rep. 5, 1–7.

Dresel, E.I.B., Moyle, V., 1950. Nitrogenous excretion in amphipods and isopods. J. Exp. Biol. 27, 210–225.

Endeward, V., Cartron, J., Ripoche, P., Gros, G., 2008. RhAG protein of the Rhesus complex is a CO2 channel in the human red cell membrane. FASEB J. 22, 64–73.

Fenton, R.A., 2009. Essential role of vasopressin-regulated urea transport processes in the mammalian kidney. Pflügers Arch. J. Physiol. 458, 169–177.

Finn, R.N., Cerdà, J., 2015. Evolution and functional diversity of aquaporins. Biol. Bull. 229, 6–23.

Freire, C.A., Onken, H., McNamara, J.C., 2008. A structure-function analysis of ion transport in crustacean gills and excretory organs. Comp. Biochem. Physiol. - A Mol. Integr. Physiol. 151, 272–304.

Gilles, R., Péqueux, A., 1981. Cell volume regulation in crustaceans: relationship between mechanisms for controlling the osmolality of extracellular and intracellular fluids. J. Exp. Zool. 215, 351–362.

Grosholz, E.D., Ruiz, G.M., 1996. Predicting the impact of introduced marine species: lessons from the multiple invasions of the European green crab *Carcinus maenas*. Biol. Conserv. 78, 59–66.

Henry, R.P., 2005. Critical salinity, sensitivity, and commitment of salinity-mediated carbonic anhydrase induction in the gills of two euryhaline species of decapod crustaceans. J. Exp. Zool. Part A Comp. Exp. Biol. 303, 45–56.

Henry, R.P., 2001. Environmentally mediated carbonic anhydrase induction in the gills of euryhaline crustaceans. J. Exp. Biol. 204, 991–1002. https://doi.org/10.1242/jeb.204.5.991

Henry, R.P., 1995. Nitrogen metabolism and excretion for cell volume regulation in invertebrates, in: Walsh, P.J., Wright, P. (Eds.), Nitrogen Metabolism and Excretion. CRC Press, Salem, pp. 63–70.

Henry, R.P., Gehnrich, S., Weihrauch, D., Towle, D.W., 2003. Salinity-mediated carbonic anhydrase induction in the gills of the euryhaline green crab, *Carcinus maenas*. Comp. Biochem. Physiol. - A Mol. Integr. Physiol. 136, 243–258.

Henry, R.P., Lucu, Č., Onken, H., Weihrauch, D., 2012. Multiple functions of the crustacean gill: Osmotic/ionic regulation, acid-base balance, ammonia excretion, and bioaccumulation of toxic metals. Front. Physiol. 3, 431.

Higgins, C., 2016. Urea and the clinical value of measuring blood urea concentration. Acutecaretesting.Org 1–6.

Hill, W.G., Mathai, J.C., Gensure, R.H., Zeidel, J.D., Apodaca, G., Saenz, J.P., Kinne-Saffran, E., Kinne, R., Zeidel, M.L., 2004. Permeabilities of teleost and elasmobranch gill apical membranes: evidence that lipid bilayers alone do not account for barrier function. Am. J. Physiol. Physiol. 287, 235–242.

Holliday, C.W., 1980. Magnesium transport by the urinary bladder of the crab, *Cancer magister*. J. Exp. Biol. 85, 187–301.

Jawed, M., 1969. Body nitrogen and nitrogenous excretion in *Neomysis rayii* Murdoch and *Euphausia pacifica* Hansen. Limnol. Ocean. 14, 748–754.

Jones, D.T., Taylor, W.R., Thornton, J.M., 1992. The rapid generation of mutation data matrices from protein sequences. Bioinformatics 8, 275–282.

Junankar, P.R., Kirk, K., 2000. Organic osmolyte channels: a comparative view. Cell. Physiol. Biochem. 10, 355–360.

Kaufmann, N., Mathai, J.C., Hill, W.G., Dow, J.A.T., Zeidel, M.L., Brodsky, J.L., 2005. Developmental expression and biophysical characterization of a *Drosophila* melanogaster aquaporin. Am. J. Physiol. Physiol. 289, 397–407.

Kikawada, T., Saito, A., Kanamori, Y., Fujita, M., Śnigórska, K., Watanabe, M., Okuda, T., 2008. Dehydration-inducible changes in expression of two aquaporins in the sleeping chironomid, *Polypedilum vanderplanki*. Biochim. Biophys. Acta - Biomembr. 1778, 514–520.

Kirschner, L.B., 2004. The mechanism of sodium chloride uptake in hyperregulating aquatic animals. J. Exp. Biol. 207, 1439–1452.

Komarova, Y., Malik, A.B., 2010. Regulation of endothelial permeability via paracellular and transcellular transport pathways. Annu. Rev. Physiol. 72, 463–493.

Krishnamoorthy, R. V., Srihari, K., 1973. Changes in excretory patterns of the freshwater field crab *Paratelphusa hydrodromus* upon adaptation to higher salinities. Mar. Biol. 21, 341–348.

Larsen, E.H., Deaton, L.E., Onken, H., O'Donnell, M.J., Grosell, M., Dantzler, W.H., Weihrauch, D., 2014. Osmoregulation and excretion. Compr. Physiol. 4, 405–573.

Li, Y., Wang, W., Jiang, T., Yang, B., 2017. Aquaporins in urinary system, in: Yang, B. (Ed.), Aquaporins. Springer Science and Business Media, Dordrecht, pp. 131–148.

Liman, E.R., Tytgat, J., Hess, P., 1992. Subunit stoichiometry of a mammalian K+ channel determined by construction of multimeric cDNAs. Neuron 9, 861–871.

Lind, U., Järvå, M., Rosenblad, M.A., Pingitore, P., Karlsson, E., Wrange, A.-L., Kamdal, E., Sundell, K.S., André, C., Jonsson, P.R., Havenhand, J., Eriksson, L.A., Hedfalk, K., Blomberg, A., 2017. Analysis of aquaporins from the euryhaline barnacle *Balanus improvisus* reveals differential expression in response to changes in salinity. PLoS One 12, e0181192.

Lucu, Č., 1989. Evidence for Cl- exchanger in perfused *Carcinus* gills. Comp. Biochem. Physiol. - A Mol. Integr. Physiol. 92, 415–420.

Lucu, Č., Siebers, D., 1987. Linkage of Cl- fluxes with ouabain sensitive Na/K exchange through *Carcinus* gill epithelia. Comp. Biochem. Physiol. - A Mol. Integr. Physiol. 87, 807–811.

Lucu, Č., Towle, D.W., 2010. Characterization of ion transport in the isolated epipodite of the lobster *Homarus americanus*. J. Exp. Biol. 213, 418–425.

Lv, J., Liu, P., Wang, Y., Gao, B., Chen, P., Li, J., 2013. Transcriptome analysis of *Portunus trituberculatus* in response to salinity stress provides insights into the molecular basis of osmoregulation. PLoS One 8, e82155.

Maddrell, S.H.P., 1964. Excretion in the blood-sucking bug, *Rhodnius Prolixus* Stal II. The normal course of diuresis and the effect of temperature. J. Exp. Biol. 41, 163–176.

Martinez, A.S., Cutler, C.P., Wilson, G.D., Phillips, C., Hazon, N., Cramb, G., 2005. Regulation of expression of two aquaporin homologs in the intestine of the European eel: Effects of seawater acclimation and cortisol treatment. Am. J. Physiol. 288, R1733–R1743.

McGaw, I.J., Curtis, D.L., 2013. A review of gastric processing in decapod crustaceans. J. Comp. Physiol. B Biochem. Syst. Environ. Physiol. 183, 443–465.

McNamara, J.C., Zanotto, F.P., Onken, H., 2005. Adaptation to hypoosmotic challenge in brachyuran crabs: A microanatomical and electrophysiological characterization of the intestinal epithelia. J. Exp. Zool. Part A Comp. Exp. Biol. 303, 880–893.

Misbah, I., Karim, M.Y., Zainuddin, Aslamyah, S., 2017. Effect of salinity on the survival of mangrove crab *Scylla tranquebarica* larvae at zoea-megalopa stages. AACL Bioflux 10, 1590–1595.

Murata, K., Mitsuoka, K., Hiral, T., Walz, T., Agre, P., Heymann, J.B., Engel, A., Fujiyoshi, Y., 2000. Structural determinants of water permeation through aquaporin-1. Nature 407, 599–605.

Nagel, H., 1934. Die aufgaben der exkretionsorgane und der kiemen bei der osmoregulation von *Carcinus Maenas*. Z. Vgl. Physiol. 21, 468–491.

Needham, A.E., 1957. Factors affecting nitrogen excretion in *Carcinus maenas* (Pennant). Physiol. Comp. et Oecologia 4, 209–239.

Neufeld, G.J., Holliday, C.W., Pritchard, J.B., 1980. Salinity adaptation of gill Na,K-ATPase in the blue crab *Callinectes sapidus*. J. Exp. Zool. 221, 215–224.

Newman, K., Aguero, T., King, M. Lou, 2018. Isolation of *Xenopus* oocytes. Cold Spring Harb. Protoc. 2018, 86–91.

Onken, H., Graszynski, K., Zeiske, W., 1991. Na+-independent, electrogenic Cl- uptake across the posterior gills of the Chinese crab (*Eriocheir sinensis*): voltage-clamp and microelectrode studies. J. Comp. Physiol. B 161, 293–301.

Onken, H., Tresguerres, M., Luquet, C.M., 2003. Active NaCl absorption across posterior gills of hyperosmoregulating *Chasmagnathus granulatus*. J. Exp. Biol. 206, 1017–1023.

Peaydee, P., Klinbunga, S., Menasveta, P., Jiravanichpaisal, P., Puanglarp, N., 2014. An involvement of aquaporin in heat acclimation and cross-tolerance against ammonia stress in black tiger shrimp, *Penaeus monodon*. Aquac. Int. 22, 1361–1375.

Pennell, J.P., Sanjana, V., Frey, N.R., Jamison, R.L., 1975. The effect of urea infusion on the urinary concentrating mechanism in protein-depleted rats. J. Clin. Invest. 55, 399–409.

Pfaffl, M.W., 2004. Quantification strategies in real-time PCR. AZ Quant. PCR 1, 89–113.

Preston, G.M., Carroll, T.P., Guggino, W.B., Agre, P., 1992. Appearance of water channels in *Xenopus* oocytes expressing red cell CHIP28 protein. Science (80-.). 256, 385–387.

Procino, G., Mastrofrancesco, L., Sallustio, F., Costantino, V., Barbieri, C., Pisani, F., Schena,

F.P., Svelto, M., Valenti, G., 2011. AQP5 is expressed in type-B intercalated cells in the collecting duct system of the rat, mouse and human kidney. Cell. Physiol. Biochem. 28, 683–692.

Prosser, L.C., Green, J.W., 1955. Ionic and osmotic concentrations in blood and urine of *Pachygrapsus crassipes* acclimated to different salinities. Biol. Bull. 109, 99–107.

Quijada-Rodriguez, A.R., Allen, G.J.P., Nash, M.T., Weihrauch, D., 2022. Postprandial nitrogen and acid-base regulation in the seawater acclimated green crab, *Carcinus maenas*. Comp. Biochem. Physiol. -Part A Mol. Integr. Physiol. 267, 111171.

Rahi, M.L., Moshtaghi, A., Mather, P.B., Hurwood, D.A., 2018. Osmoregulation in decapod crustaceans: physiological and genomic perspectives. Hydrobiologia 825, 177–188.

Rahmatullah, M., Boyde, T.R.C., 1980. Improvements in the determination of urea using diacetyl monoxime; methods with and without deproteinisation. Clin. Chim. acta 107, 3–9.

Rao, Y., Jan, L.Y., Jan, Y.., 1990. Similarity of the product of the Drosophila neurogenic gene big brain to transmembrane channel proteins. Nat. 345, 163–167.

Rathmayer, M., Siebers, D., 2001. Ionic balance in the freshwater-adapted Chinese crab, *Eriocheir sinensis*. J. Comp. Physiol. - B Biochem. Syst. Environ. Physiol. 171, 271–281.

Riestenpatt, S., Onken, H., Siebers, D., 1996. Active absorption of Na+ and Cl-across the gill epithelium of the shore crab *Carcinus maenas*: voltage-clamp and ion-flux studies. J. Exp. Biol. 199, 1545–1554.

Rivera-Ingraham, G.A., Lignot, J.H., 2017. Osmoregulation, bioenergetics and oxidative stress in coastal marine invertebrates: raising the questions for future research. J. Exp. Biol. 220, 1749–1760.

Rojek, A., Praetorius, J., Frøkiaer, J., Nielsen, S., Fenton, R.A., 2008. A current view of the mammalian aquaglyceroporins. Annu. Rev. Physiol. 70, 301–327.

Sales, A.D., Lobo, C.H., Carvalho, A.A., Moura, A.A., Rodrigues, A.P.R., 2013. Structure, function, and localization of aquaporins: Their possible implications on gamete cryopreservation. Genet. Mol. Res. 12, 6718–6732.

Siebers, D., Leweck, K., Markus, H., Winkler, A., 1982. Sodium regulation in the shore crab

Carcinus maenas as related to ambient salinity. Mar. Biol. 69, 37–43.

Siebers, D., Lucu, Č., Winkler, A., Grammerstorf, U., Wille, H., 1987. Effects of amiloride on sodium chloride transport across isolated perfused gills of shore crabs *Carcinus maenas* acclimated to brackish water. Comp. Biochem. Physiol. -Part A Mol. Integr. Physiol. 87, 333–340.

Siebers, D., Winkler, A., Leweck, K., Madian, A., 1983. Regulation of sodium in the shore crab *Carcinus maenas*, adapted to environments of constant and changing salinities. Helgolander Meeresunters 36, 303–312.

Siebers, D., Winkler, A., Lucu, Č., Thedens, G., Weichart, D., 1985. Na-K-ATPase generates an active transport potential in the gills of the hyperregulating shore crab *Carcinus maenas*. Mar. Biol. 87, 185–192.

Simonik, E., Henry, R.P., 2014. Physiological responses to emersion in the intertidal green crab, *Carcinus maenas* (L.). Mar. Freshw. Behav. Physiol. 47, 101–115.

Sohara, E., Rai, T., Miyazaki, J.I., Verkman, A.S., Sasaki, S., Uchida, S., 2005. Defective water and glycerol transport in the proximal tubules of AQP7 knockout mice. Am. J. Physiol. - Ren. Physiol. 289, F1195–F1200.

Soupene, E., Inwood, W., Kustu, S., 2004. Lack of the Rhesus protein Rh1 impairs growth of the green alga *Chlamydomonas reinhardtii* at high CO2. Proc. Natl. Acad. Sci. U. S. A. 101, 7787–7792.

Stanley, J.G., Fleming, W.R., 1964. Excretion of Hypertonic Urine by a Teleost. Science (80-.). 144, 63–64.

Stavang, J.A., Chauvigné, F., Kongshaug, H., Cerdà, J., Nilsen, F., Finn, R.N., 2015. Phylogenomic and functional analyses of salmon lice aquaporins uncover the molecular diversity of the superfamily in Arthropoda. BMC Genomics 16, 618.

Su, W., Cao, R., Zhang, X., Guan, Y., 2020. Aquaporins in the kidney: physiology and pathophysiology. Am J Physiol Ren. Physiol 318, 193–203.

Sui, H., Han, B.G., Lee, J.K., Walian, P., Jap, B.K., 2001. Structural basis of water-specific transport through the AQP1 water channel. Nature 414, 872–878.

Tani, K., Mitsuma, T., Hiroaki, Y., Kamegawa, A., Nishikawa, K., Tanimura, Y., Fujiyoshi, Y., 2009. Mechanism of aquaporin-4's fast and highly selective water conduction and proton exclusion. J. Mol. Biol. 389, 694–706.

Tatsumi, K., Tsuji, S., Miwa, H., Morisaku, T., Nuriya, M., Orihara, M., Kaneko, K., Okano, H., Yasui, M., 2009. *Drosophila* big brain does not act as a water channel, but mediates cell adhesion. FEBS Lett. 583, 2077–2082.

Thies, A.B., Quijada-Rodriguez, A.R., Zhouyao, H., Weihrauch, D., Tresguerres, M., 2022. A rhesus channel in the coral symbiosome membrane suggests a novel mechanism to regulate NH3 and CO2 delivery to algal symbionts. Sci. Adv. 8.

Tipsmark, C.K., Sørensen, K.J., Madsen, S.S., 2010. Aquaporin expression dynamics in osmoregulatory tissues of Atlantic salmon durings moltification and seawater acclimation. J. Exp. Biol. 213, 368–379.

Towle, D.W., Weihrauch, D., 2001. Osmoregulation by gills of euryhaline crabs: molecular analysis of transporters. Am. Zool. 41, 770–780.

Truchot, J.-P., 1988. Problems of acid-base balance in rapidly changing intertidal environments. Am. Zool. 28, 55–64.

Tsai, J.R., Lin, H.C., 2014. Functional anatomy and ion regulatory mechanisms of the antennal gland in a semi-terrestrial crab, *Ocypode stimpsoni*. Biol. Open 3, 409–417.

Wang, X., Wang, S., Li, C., Chen, K., Qin, J.G., Chen, L., Li, E., 2015. Molecular Pathway and Gene Responses of the Pacific White Shrimp *Litopenaeus vannamei* to Acute Low Salinity Stress. J. Shellfish Res. 34, 1037–1048.

Weihrauch, D., Becker, W., Postel, U., Luck-Kopp, S., Siebers, D., 1999a. Potential of active excretion of ammonia in three different haline species of crabs. J. Comp. Physiol. B 169, 25–37.

Weihrauch, D., Siebers, D., Towle, D.W., 1999b. High levels of urea maintained in the hemolymph, in: Hochachka, P.W., Mommsen, T.P. (Eds.), Fifth International Congress of Comparative Physiology and Biochemistry. Elsevier, Calgary, Alberta, p. S81.

Weihrauch, D., Wilkie, M.R., Walsh, P.J., 2009. Ammonia and urea transporters in gills of fish and aquatic crustaceans. J. Exp. Biol. 212, 1716–1730.

Wheatly, M.G., Henry, R.P., 1987. Branchial and antennal gland Na+/K+-dependent ATPase and carbonic anhydrase activity during salinity acclimation of the euryhaline crayfish *Pacifastacus leniusculus*. J. Exp. Biol. 133, 73–86.

Whittamore, J.M., 2012. Osmoregulation and epithelial water transport: lessons from the intestine of marine teleost fish. J. Comp. Physiol. B Biochem. Syst. Environ. Physiol. 182, 1–39.

Wilson, J.M., 2007. The use of immunochemistry in the study of branchial ion transport mechanisms, in: Baldisserotto, B., Mancera, J.M., Kapoor, B.G. (Eds.), Fish Osmoregulation. Science Publishers, New Hampshire, pp. 359-394.

Winkler, A., Siebers, D., Becker, W., 1988. Osmotic and ionic regulation in shore crabs *Carcinus maenas* inhabiting a tidal estuary. Helgolander Meeresunters 42, 99–111.

Yancey, P.H., 2001. Water stress, osmolytes and proteins. Am. Zool. 41, 699–709.

Yang, B., 2017. Aquaporins. Springer Nature, Dordrecht.

Yanochko, G.M., Yool, A.J., 2002. Regulated cationic channel function in *Xenopus* oocytes expressing Drosophila Big Brain. J. Neurosci. 22, 2530–2540.

Yasui, M., Kwon, T.H., Knepper, M.A., Nielsen, S., Agre, P., 1999. Aquaporin-6: an intracellular vesicle water channel protein in renal epithelia. Proc. Natl. Acad. Sci. U. S. A. 96, 5808–5813.

7.0 Appendices

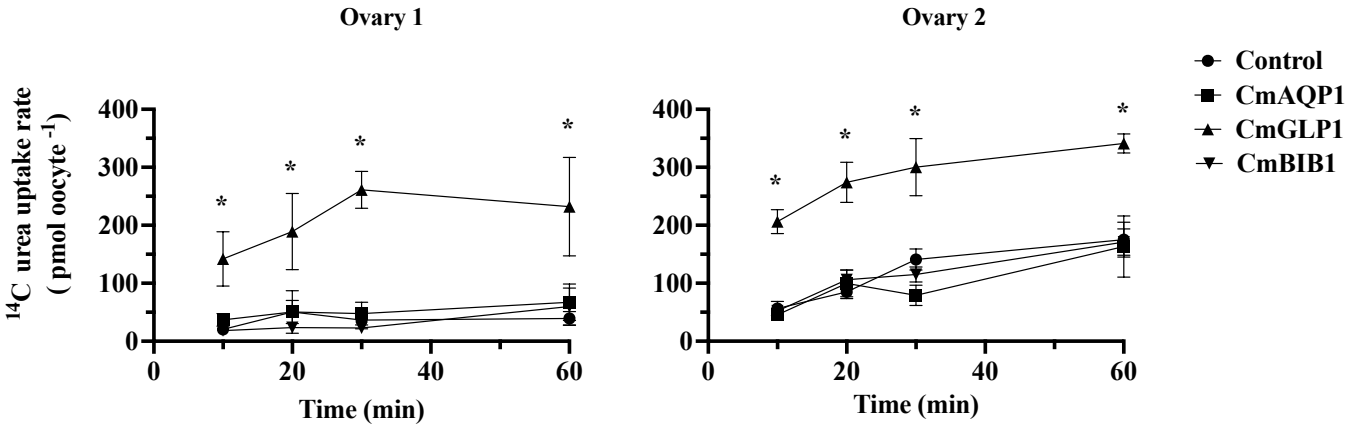

Figure 14: Uptake of ^{14}C urea in *Xenopus laevis* oocytes expressing *Carcinus maenas* aquporins: CmAQP1, CmGLP1, and CmBIB1 after either a 10, 20, 30, or 60-minute incubation in media containing 1 mmol l^{-1} urea and 1 μCi ml^{-1} ^{14}C-urea. Asterisks denote significant differences between control and CmGLP1 expressing oocytes (Two-way ANOVA, Dunnet's $P < 0.0001$, n = 6-9 oocytes).

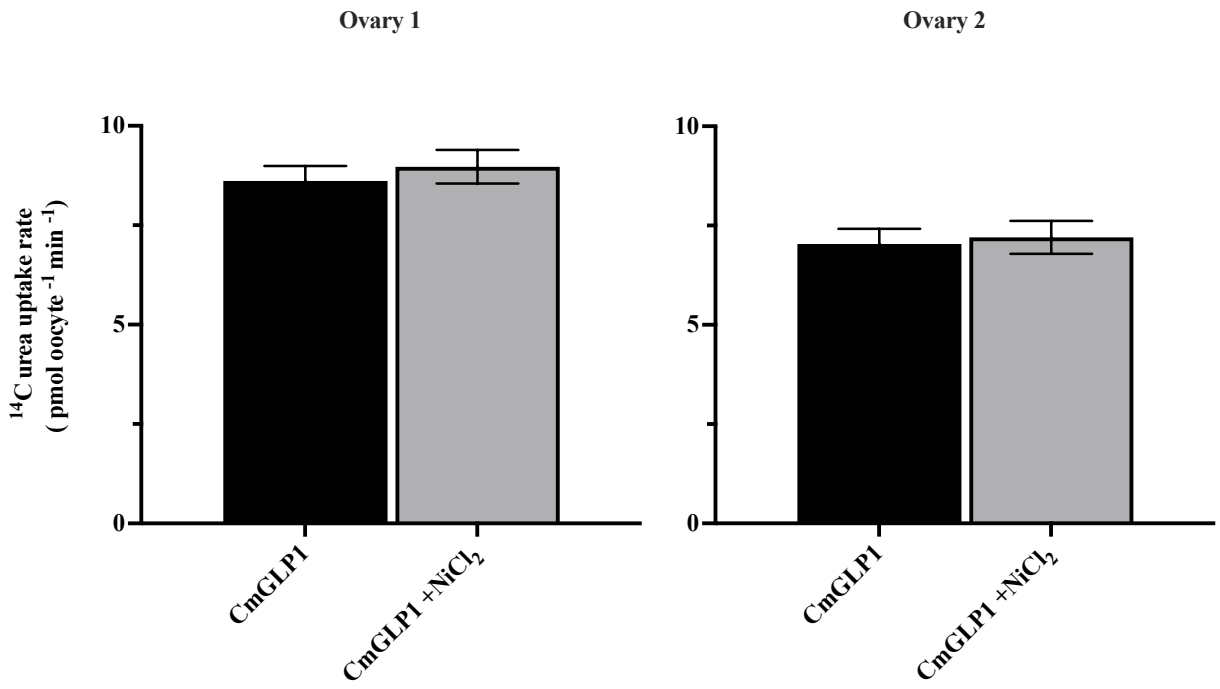

Figure 15: Uptake of ^{14}C urea in *Xenopus laevis* oocytes expressing *Carcinus maenas* GLP1. Oocytes were incubated in OR2 containing 1 mmol l^{-1} $NiCl_2$ for 1 hour prior to ^{14}C exposure. Oocytes were then incubated for 30 minutes in OR2 containing 1 mmol l^{-1} $NiCl_2$, 1 mmol l^{-1} urea and 1 µCi ml^{-1} ^{14}C-urea. Positive fluxes indicate ^{14}C-urea uptake. Control ^{14}C-urea fluxes subtracted from CmGLP1 fluxes (n = 10-12 oocytes). Student's T-test indicated no significant uptake differences between oocytes expressing CmGLP1 with or without $NiCl_2$ treatment.

Table 1: Primers used in the amplification of *Carcinus maenas* aquaporins- CmAQP1, CmGLP1, CmBIB1, elongation factor one-alpha (EF1α), and ribosomal protein S3 (RPS3) for qPCR assays.

Transcript	Primer (5'→ 3')	Annealing Temperature	Product size (bp)	GenBank accession no.
Classical AQP *(CmAQP Fy/Ry)*	*Sense:* GCTCTACATCATCGCCCAGT *Antisense:* GAACACAGTCAGCACGAGGA	58	178	GBXE01030866.1
Aquaglyceroporin *(CmAQP10 qPCR F1/R1)*	*Sense:* GGTGTGTTTCGGCTTCAACT *Antisense:* AGCGCTGAACGTGTCACTAC	56	106	GBXE01131729.1
Big brain protein *(CmAQP-like a qPCR F1/R1)*	*Sense:* CCTGTCCACAGTGCTGGTAA *Antisense:* CAATATGAGCCGTGGTGATG	60	116	GFXF01046256.1
Ribosomal protein subunit 8 *(CmRPL8 F1/R1)*	Sense: AACGTGATGCCCATCGGAAC Antisense: TCACCCTGGTCTTCTTGGTCTC	60	148	GBXE01030575.1
Elongation factor 1-α *(CmEF1α* F1/R1)	Sense: CAACAAGATGGACAGCACGGAG Antisense: ATGGGAAGGATTGGCACGATGG	60	123	GFYW01048882.1

Table 2: Primers employed for obtaining the open reading frames and cloning CmAQP1, CmGLP1, and CmBIB1 into the pGEM-HE vector.

Transcript	Primer (5'→ 3')	Annealing Temperature	Product size (bp)	GenBank accession no.
Classical AQP *(CmAQP ORF F1/R1)*	*Sense:* ATGGGCAAGATTAAGGATACCC *Antisense:* TTAGGGTTGGTTGGCTCTCT	54.2°C	780	GBXE01030866.1
Classical AQP *(CmAQP BamH1/Hind3)*	*Sense: BAMH1* AAAGGATCCATGGGCAAGATTAAGGA *Antisense:* HIND3 AAAAAGCTTTTAGGGTTGGTTGGCTCTCT	58.9°C	820	GBXE01030866.1
Big brain protein *(CmAQP-like a ORF F2/R2)*	*Sense:* TCCCACGCTCTCTCTCTCTC *Antisense:* AGTGTGCGTCAAGACAGTGG	67°C	1112	GBXE01131729.1
Big brain protein *(CmAQP-like a ECOR1F/ HindIIIR)*	*Sense:*ECOR1 AAAAGAATTCATGCCAATACTAGATGGAGA *Antisense:* Hind3 AAAAAAGCTTTTAGCAGGGGGATGCC	65°C	1034	GBXE01131729.1
Aquaglyceroporin *(CrabORF AQP10 F/RA*)	*Sense:* ATGGGNAACGCNAAGNTNGTCGARGC *Antisense:* GTGATAGTGCCTGGGTAGGTGGC	45°C	446	GFBL01038362.1 GFFJ01052468.1 GBXE01131729.1
Aquaglyceroporin *(CmAQP9 F1/ CmAQP10 ORF R1*)	*Sense:* GTTTACTTGAACGCCCTGGA *Antisense:* CTAATCAGAAGGTTTGACAG	45°C	570	ON416880
Aquaglyceroporin *(CmAQP10 SmalF/ XbalR*)	*Sense: SMAL* AAAACCCGGGATGGGGAACGCAAAGTT *Antisense: XBAL* TTTTTCTAGACTAATCAGAAGGTTTGACAG	60°C	950	ON416880

Table 3: Accession numbers of sequences included in the Maximum likelihood analysis in figure 8. References: [1]Campbell et al., 2008; [2]Lind et al., 2017; [3]Chung et al., 2012; [4]Yang, 2017; [5]Stavang et al., 2015; [6]Peaydee et al., 2014; [7]Lv et al., 2013. Columns without literature were obtained through mining transcriptomes using Genbank blast of crustacean species employing *C. maenas* AQP sequences obtained in this study.

Species name	Ortholog Name	Amino Acid Genbank Accession No.	Literature
Aedes aegypti	AQP	AAF64037.1	1
Aedes aegypti	PRIP	XP_001656932	1
Aedes aegypti	BIB	XP_001649747	1
Aedes aegypti	DRIP	AF218314	1
Apis mellifera	DRIP	XP_624531	1
Apis mellifera	PRIP	XP_394391	1
Apis mellifera	BIB	XP_396705	1
Balanus improvisus	AQP1	ARA90634.1	2
Balanus improvisus	AQP2	ARA90637.1	2
Balanus improvisus	BIB	ARA90640.1	2
Balanus improvisus	BIBL1	ARA90641.1	2
Balanus improvisus	BIBL2	ARA90644.1	2
Balanus improvisus	GLP1	ARA90645.1	2
Balanus improvisus	GLP2	ARA90646.1	2
Balanus improvisus	AQP12	ARA90647.1	2
Bombyx mori	DRIP	BAD69569	1
Callinectes sapidus	AQP1	AFR36904.1	3
Carcinus maenas	AQP1	ON416879	
Carcinus maenas	GLP1	ON416880	
Carcinus maenas	BIB1	ON416881	
Chionoecetes opilio	AQP	KAG0710491.1	
Cicadella viridis	AQP	Q23808	1
Daphnia magna	AQP7	XP_045025567.1	
Daphnia magna	AQP	KZS10587.1	
Drosophila melanogaster	PRIP	NP_610686	1
Drosophila melanogaster	BIB	AAF52844	1
Drosophila melanogaster	DRIP	AAA81324.1	1
Haematobia irritans	DRIP	AAA96783	1
Homarus americanus	AQP	XP_042221791.1	
Homo sapiens	AQP0	NP_036196.1	4
Homo sapiens	AQP1	NP_001316801.1	4
Homo sapiens	AQP2	NP_000477.1	4
Homo sapiens	AQP3	NP_004916.1	4
Homo sapiens	AQP4	NP_001304313.1	4
Homo sapiens	AQP5	NP_001642.1	4
Homo sapiens	AQP6	NP_001643.2	4
Homo sapiens	AQP7	NP_001161.1	4
Homo sapiens	AQP8	NP_001160.2	4

Homo sapiens	AQP9	NP_066190.2	4
Homo sapiens	AQP10	NP_536354.2	4
Homo sapiens	AQP11	NP_766627.1	4
Homo sapiens	AQP12	NP_945349.1	4
Lepeophtheirus salmonis	BIB	ALA27395.1	5
Lepeophtheirus salmonis	Glp1_v1	ADD38378.1	5
Lepeophtheirus salmonis	Glp1_v2	ALA27398.1	5
Lepeophtheirus salmonis	Glp2	ALA27399.1	5
Lepeophtheirus salmonis	Glp3_v1	ALA27400.1	5
Lepeophtheirus salmonis	Glp3_v2	ALA27401.1	5
Lepeophtheirus salmonis	AQP12L1	ALA27402.1	5
Lepeophtheirus salmonis	AQP12L2	ALA27403.1	5
Lutzomyia longipalpis	AQP	ABV60346	1
Macrobrachium rosenbergii	AQP	AET34919.1	
Penaeus japonicus	AQP	XP_042880267.1	
Penaeus monodon	AQP	XP_037778323.1	6
Penaeus vannamei	AQP	ANO39146.1	
Pollicipes pollicipes	AQP	XP_037085117.1	
Portunus trituberculatus	AQP	AHB64460.1	7
Polypedilum vanderplanki	PRIP	BAF62090.1	1
Pyrocoelia rufa	AQP1	AAL09065	1
Tribolium castaneum	DRIP	XP_972862	1
Tribolium castaneum	BIB	XP_968782	1
Trinorchestia longiramus	AQP	KAF2355402.1	1